IN-SITU MICROSCOPIC
STUDIES OF DEFORMATION

Richard Campbell
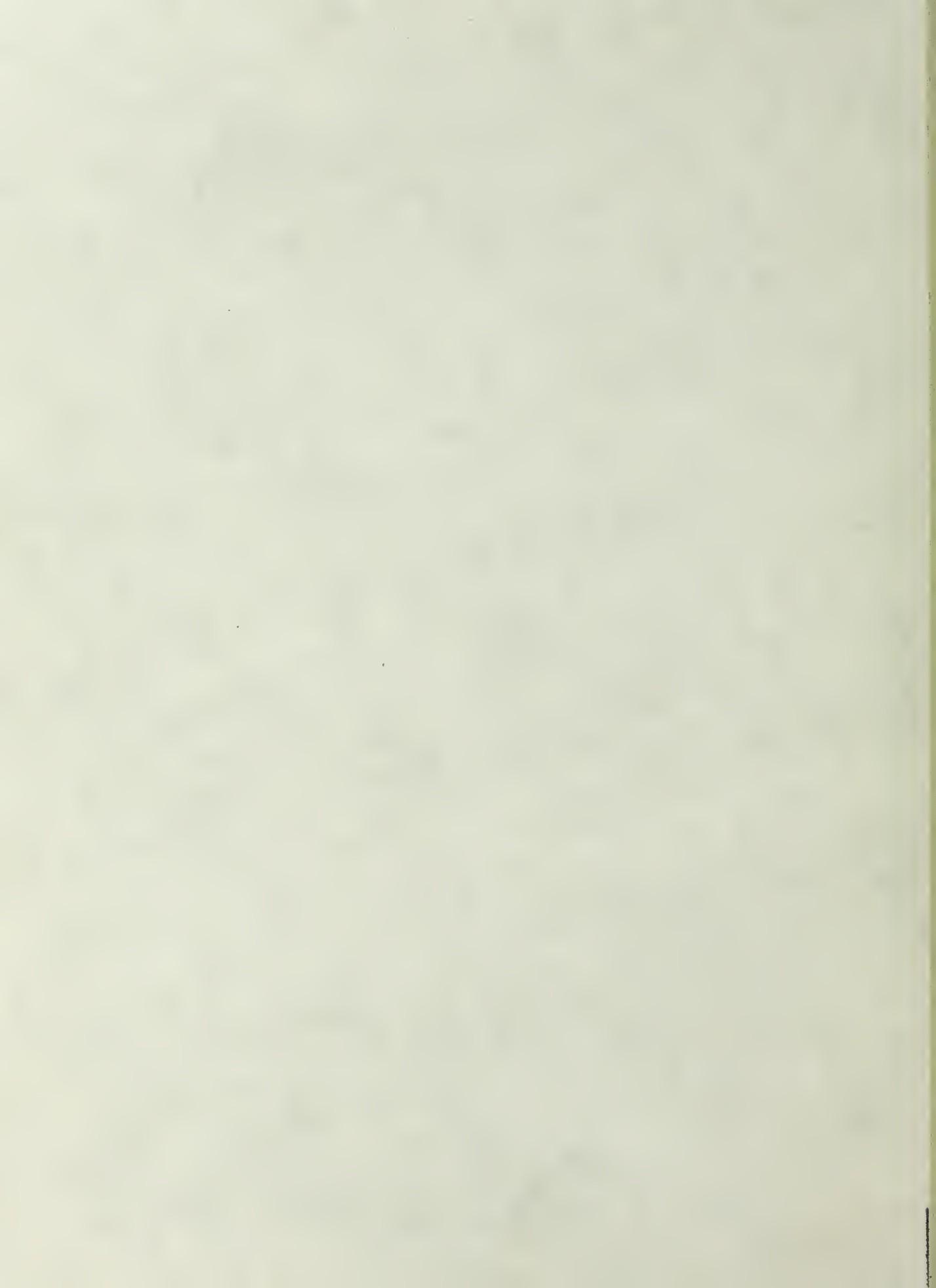
NAVAL POSTGRADUATE SCHOOL
Monterey, California

THESIS

IN-SITU MICROSCOPIC STUDIES OF DEFORMATION

by

Richard Campbell

March 1981

Thesis Advisor   J. Perkins

Approved for public release, distribution unlimited

SECURITY CLASSIFICATION OF THIS PAGE (When Data Entered)

REPORT DOCUMENTATION PAGE		READ INSTRUCTIONS BEFORE COMPLETING FORM
1. REPORT NUMBER	2. GOVT ACCESSION NO.	3. RECIPIENT'S CATALOG NUMBER
4. TITLE (and Subtitle) In-Situ Microscopic Studies of Deformation		5. TYPE OF REPORT & PERIOD COVERED Master's Thesis March 1981
		6. PERFORMING ORG. REPORT NUMBER
7. AUTHOR(s) Richard Campbell		8. CONTRACT OR GRANT NUMBER(s)
9. PERFORMING ORGANIZATION NAME AND ADDRESS Naval Postgraduate School Monterey, California 93940		10. PROGRAM ELEMENT, PROJECT, TASK AREA & WORK UNIT NUMBERS
11. CONTROLLING OFFICE NAME AND ADDRESS Naval Postgraduate School Monterey, California 93940		12. REPORT DATE March 1981
		13. NUMBER OF PAGES 77
14. MONITORING AGENCY NAME & ADDRESS(If different from Controlling Office)		15. SECURITY CLASS. (of this report) Unclassified
		15a. DECLASSIFICATION/DOWNGRADING SCHEDULE

16. DISTRIBUTION STATEMENT (of this Report)

Approved for public release; distribution unlimited.

17. DISTRIBUTION STATEMENT (of the abstract entered in Block 20, if different from Report)

18. SUPPLEMENTARY NOTES

19. KEY WORDS (Continue on reverse side if necessary and identify by block number)

Scanning Electron Microscope
power-screw-pairs
parallel cross-head

20. ABSTRACT (Continue on reverse side if necessary and identify by block number)

The design and construction of an experimental strain/heating stage for the Cambridge Stereoscope Scanning Electron Microscope is reported. The stage is of the parallel cross-head type driven by opposed power-screw-pairs. Complete machine drawings for the major components of the stage are included. The design has been tested by carrying out experiments on shape-memory-effect alloys and annealed brass specimens.

DD FORM 1473 JAN 73   EDITION OF 1 NOV 68 IS OBSOLETE
S/N 0102-014-6601 |

In-Situ Microscopic Studies of Deformation

by

Richard Campbell
Lieutenant Commander, United States Navy
B.S.M.E., University of Idaho, 1972

Submitted in partial fulfillment of the
requirements for the degree of

MASTER OF SCIENCE IN MECHANICAL ENGINEERING

from the

NAVAL POSTGRADUATE SCHOOL
March 1981

ABSTRACT

The design and construction of an experimental strain/
heating stage for the Cambridge Stereoscope Scanning
Electron Microscope is reported. The stage is of the
parallel cross-head type driven by opposed power-screw pairs.
Complete machine drawings for the major components of the
stage are included. The design has been tested by carrying
out experiments on shape-memory-effect alloys and annealed
brass specimens.

TABLE OF CONTENTS

LIST OF FIGURES

NOMENCLATURE

ENGLISH LETTER SYMBOLS

A_b	Bearing stress area	[in²]
A_r	Minor Diameter area	[in²]
A_s	Shear stress area	[in²]
A_t	Tensile stress area	[in²]
d	Nominal diameter	[in]
d_c	Collar diameter	[in]
d_a	Gear Pitch diameter	[in]
d_m	Mean diameter	[in]
d_r	Minor diameter	[in]
E	Young's Modulus of Elasticity	[psi]
F	Force	[lbf]
F_a	Axial force	[lbf]
F_n	Normal force	[lbf]
F_s	Shear force	[lbf]
L,l	Length	[in]
M	Moment	[in-lbf]
N	Number of threads per inch	$[\frac{Threads}{in}]$
n	Factor of Safety	[unitless]
P	Pitch	$[\frac{in}{Thread}]$
SEM	Scanning Electron Microscope	
ss	Stainless steel	
T/C	Thermocouple	

-

7

T_{TR}	Torque to Rotate	[in-lbf]
UNC	Unified National Coarse	
UNF	Unified National Fine	
W	Gear force	[lbf]

GREEK LETTER SYMBOLS

δ	Deflection	[in]
ε	Strain	[in/in]
θ	Slope	[in/in]
λ	Lead angle	[degrees]
μ	Coefficient of friction	[unitless]
σ_{uts}	Ultimate tensile stress	[psi]
σ_{ys}	Yield stress in shear	[psi]
σ_{yt}	Yield stress in tension	[psi]
τ	Shear stress	[psi]
ϕ_n	Pressure angle	[degrees]
ψ	Helix angle	[degrees]
2α	thread angle	[degrees]

ACKNOWLEDGEMENT

I. INTRODUCTION

For many years, shape-memory-effect materials have been
a laboratory curiosity. However, recent developments have
aroused engineering interest.

Through work sponsored by the International Copper Re-
search Association, a new family of brasses has been developed.
This Cu-Zn-Al family has the distinct property of reliable
reproduction of shape-memory-effects at transformation
temperatures up to 120°C.

A side effect of the shape-memory alloy is the ability
to do work. When a shape-memory-effect alloy is deformed
(strained about 9%) and then heated through its transformation
temperature range, it returns to its original shape and in
doing so is capable of doing work. In fact, it is capable of
doing significantly more work than was required to deform it,
thus leading to the possibility of numerous engineering appli-
cations such as the shape-memory-effect alloy heat engine
[Ref. 14]. Note that this is because it stores and converts
thermal energy.

In order to fully understand the transformation mechanisms
during the deformation and reversion, it is desirable to
monitor the microscopic processes using a scanning electron
microscope (SEM). The Material Science Department Laboratory
at the Naval Postgraduate School is equipped with a Cambridge

Stereoscan SEM and the Cambridge Corporation offers a variety
of stages for use with their machine. Unfortunately, while
they offer a heating and cooling stage and a tensile specimen
stage, the Cambridge Corporation does not presently produce
a stage capable of straining and heating a specimen at the
same time, which is a necessity for the study of shape-memory-
effect alloys. Therefore, the remainder of this paper deals
with the design considerations, fabrication and testing of
such a stage in order to disclose the observed phenomena of
the shape-memory-effect alloys.

II. DESIGN CONSIDERATIONS

Important design factors fall into two categories: (1)
Limitations of the Cambridge Stereoscan (Scanning Electron
Microscope) SEM; and (2) desired specimen environment (i.e.
temperature and strain).

A. CAMBRIDGE STEREOSCAN LIMITATIONS

Careful scrutiny of technical manuals and prints of the
Cambridge SEM set the maximum vacuum chamber operating temper-
ature at 400°C to prevent damage to nylon gear components.
The maximum outside dimensions of the strain/heating stage
to be installed are: 1) 4" in length and 3" in width to
permit sufficient x/y movement for centering a specimen and
2) 2.5" in height to permit entre of a 3" wide stage into
the 5" diameter vacuum chamber access port.

In addition to the foregoing limitations, since a torque
will be externally applied through the θZ or θZ' control,
stress limitations must be calculated. The weakest structure
in the θZ and θZ' control system is the extending drive
(Figures 1, 2 and 3). The maximum torque was determined as
follows:

From Figure 3:

12
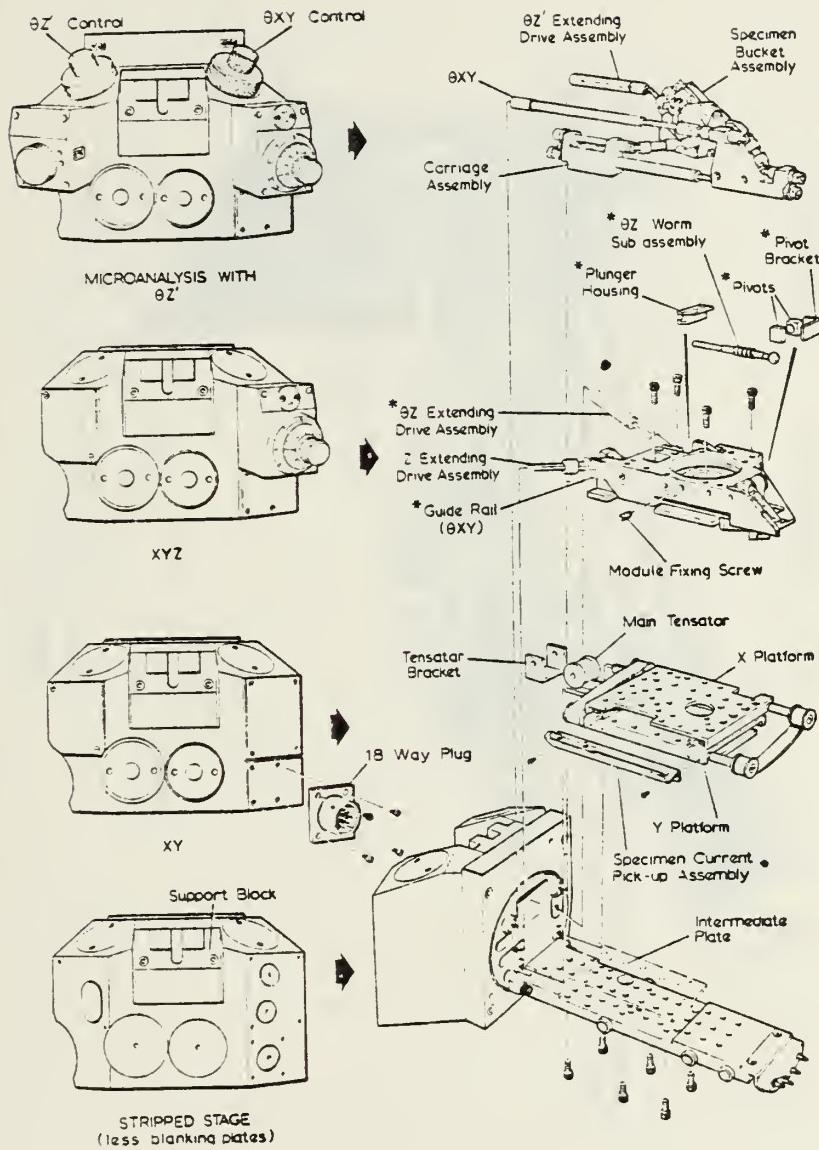
Figure 1. Cambridge microanalysis stage

13

Locking Screws For
Counter Drive Assemblies

ΘXY Carriage Assembly

Bucket Assembly (One
Standards Block Removed)

ΘZ' Extending Drive

ΘZ Extending Drive

Figure 2.   ΘZ/ΘZ' extension

14
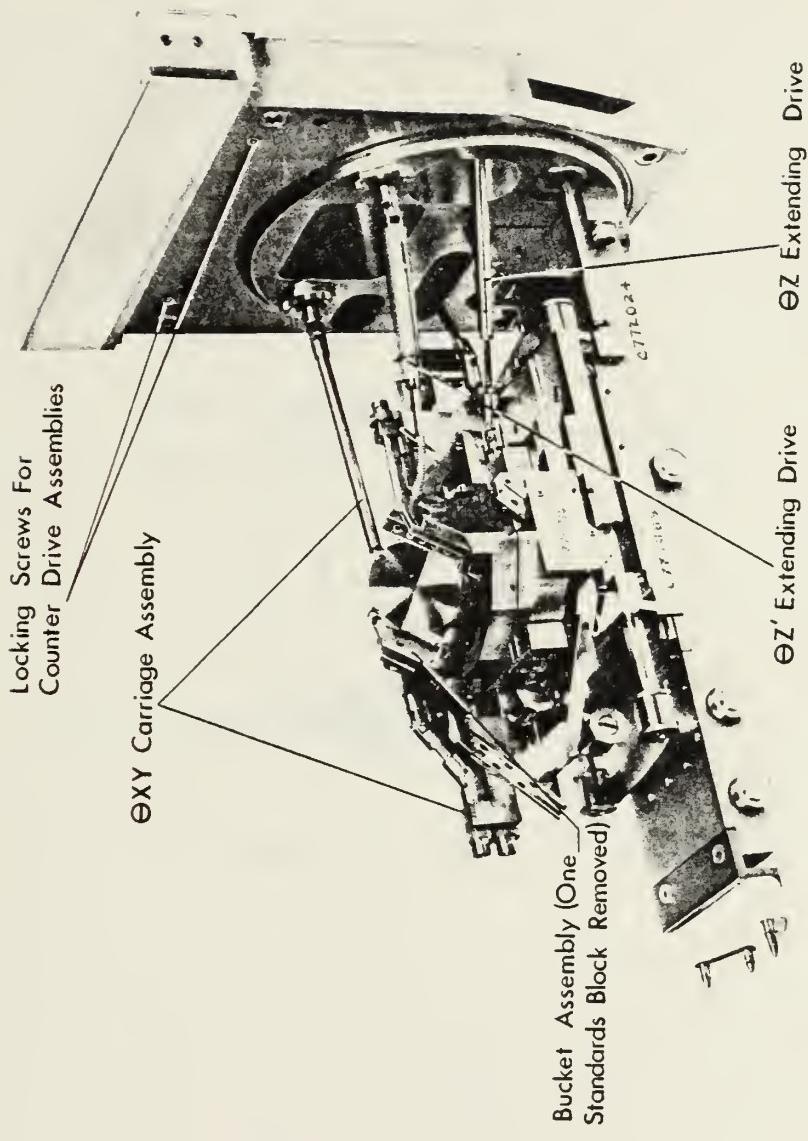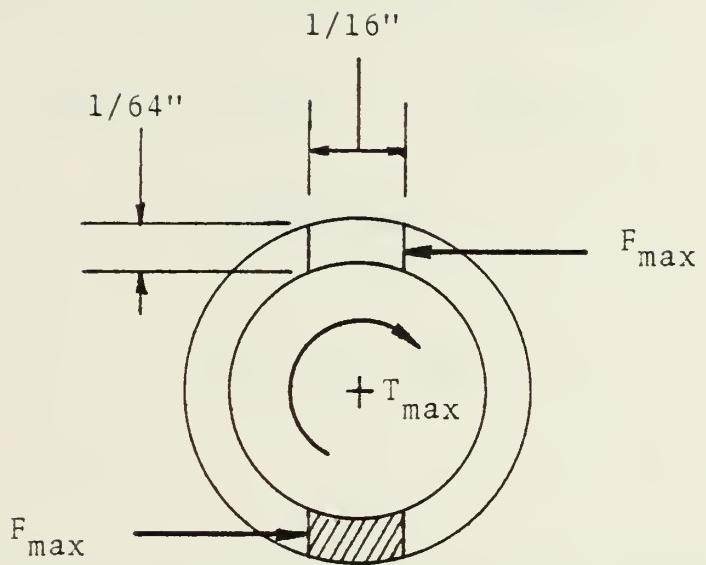
Figure 3. Force diagram of extension

Let $\qquad\sigma_{YS} = \dfrac{\sigma_{Yt}}{2} = 20 \times 10^{3} \; psi$

But $\qquad\sigma_{YS} \doteq \dfrac{F_{max}}{A_s}$

Thus $\qquad F_{max} = \sigma_{YS} A_s = 19.5 \; lbf$

So for the couple shown, summing the moments

$$T_{max} = 2 F_{max} r = F_{max} d$$

$$= (19.5)\left(\dfrac{3}{16}\right)$$

$$= 3.7 \; in\text{-}lbf$$

Lastly, to minimize interference with the electron beam, vacuum chamber materials must be non-magnetic.

B. STAGE DESIGN CONSIDERATIONS

Obviously, this section must answer the question: What is expected of the strain/heating stage? Based on the desires and recommendations of the research personnel who expect to utilize the stage, the following requirements are set forth:

(1) Maximum specimen size: 0.50 x 0.25 x 0.040 in

(2) Minimum specimen gage length: 0.25 in

(3) Maximum tensile loading: 50 lbf

16

(4) Stress level readout

(5) Operating temperature range: 25°C-120°C

(6) Temperature readout

(7) Sensitive elongation control

(8) Elongation readout

III. GENERAL ARRANGEMENT

Figure 4 shows the strain/heating stage assembly. The opposed power-screw pair are driven by rotating the $\theta Z'$ (θZ) control knob. Digital read out for this knob is provided. An increase of 1 increment on the digital readout for the $\theta Z'$ control corresponds to a cross-head separation increase of 0.0005 in ± 0.00025 (0.0004 in ± 0.0002 for θZ control). The rotation of the $\theta Z'$ (θZ) control knob results in an applied torque to the $\theta Z'$ (θZ) extension.

By means of a universal joint coupling, the applied torque is transmitted to the 48 pitch, single thread, Boston Gear steel worm and bronze worm gear assembly pair. The 20:1 reduction gear assembly has a maximum output torque capability of 37 in-lbf per power-screw, if one assumes 100% efficiency and a maximum torque input of 3.7 in-lbf for the worm and worm gear assembly pair.

Since each worm gear is securely fastened to its associated power-screw by means of counter sunk set screws, the output torque is transmitted directly to the power-screw pair. As the 1/4 - 20 UNC power-screws rotate clockwise, the cross-heads separate. For a specimen securely fastened between the two cross-heads by the hold-downs, this elongation enduces a tensile stress.

18
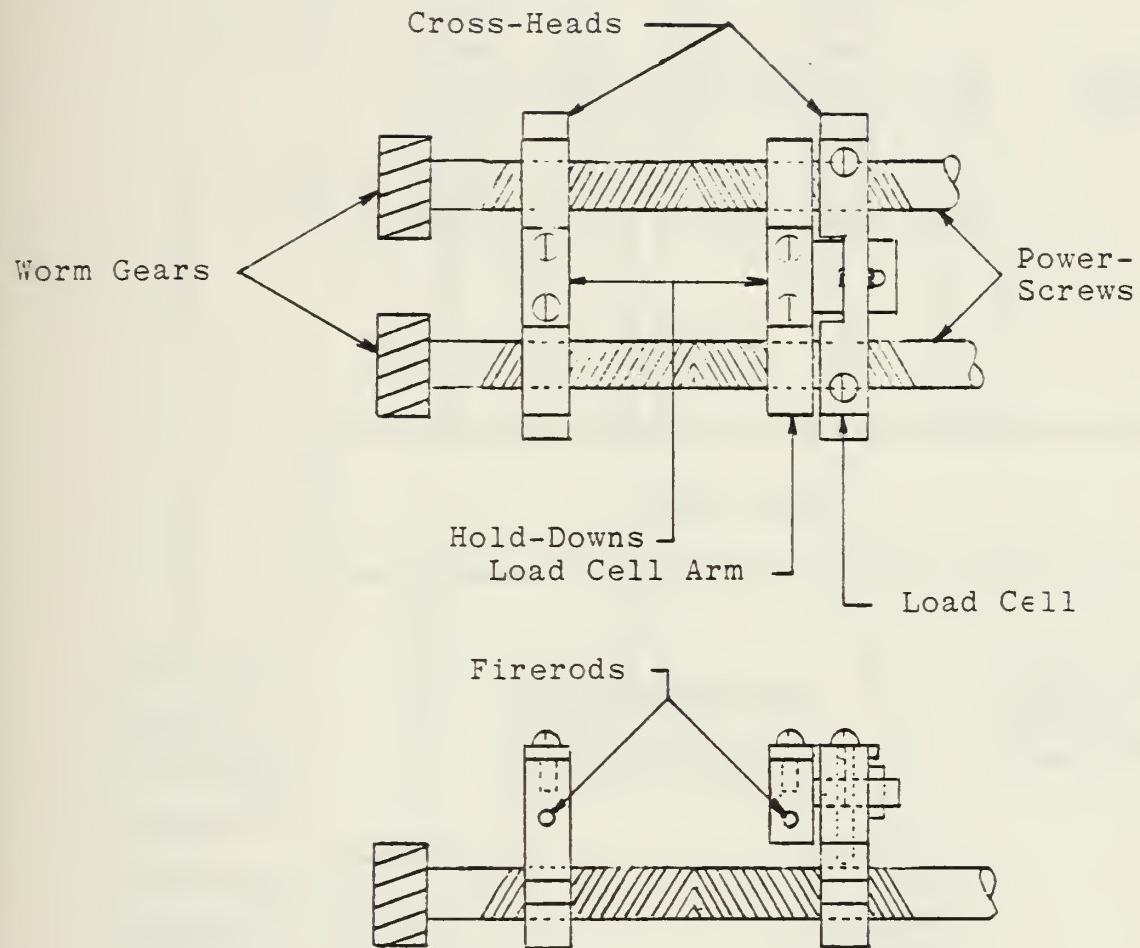
Figure 4. Strain/heating stage assembly

19
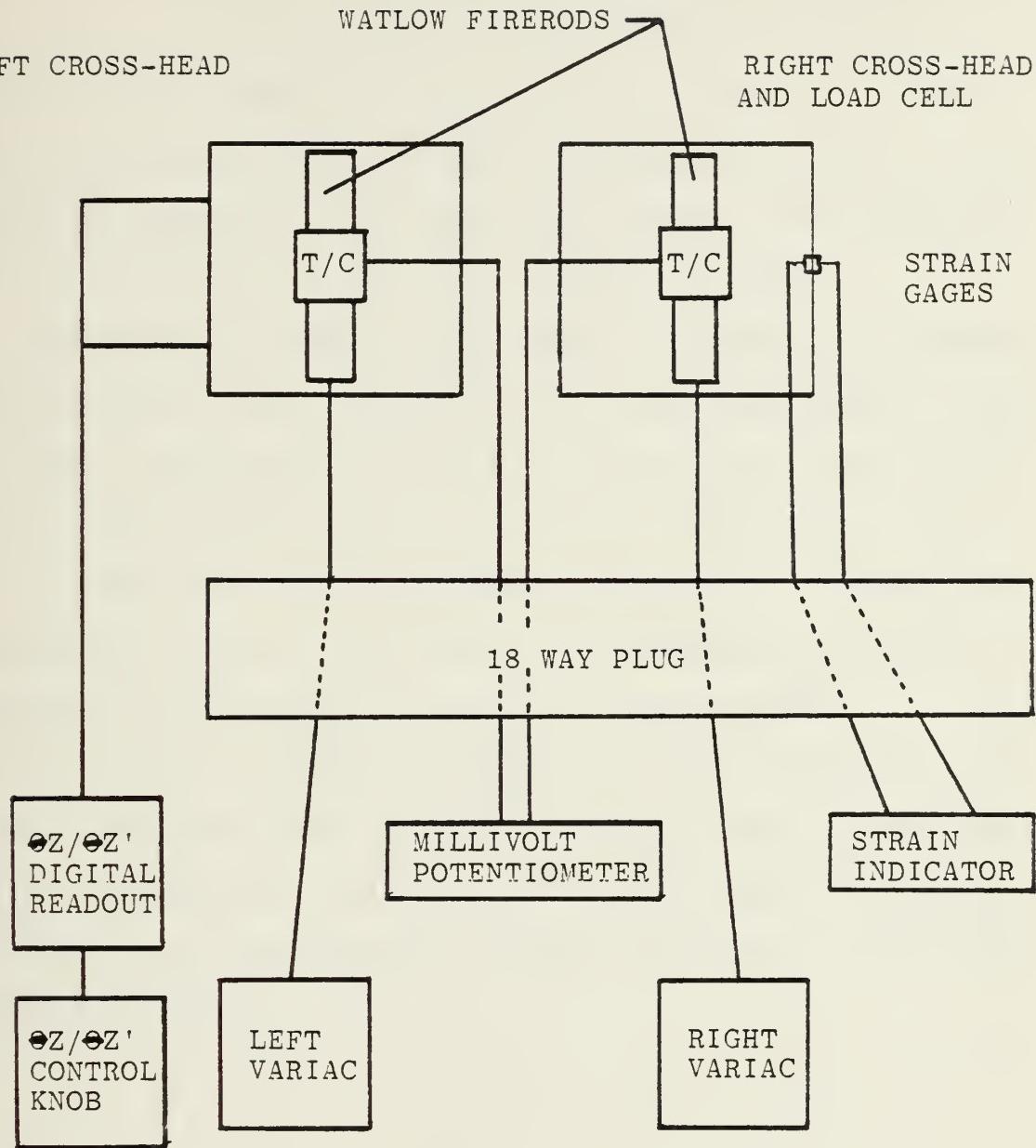
Figure 5. Schematic diagram of stage assembly.

As the specimen is elongated the tensile stress is trans-
mitted from the load cell arm to the temperature compensated
load cell. Load cell readout is then obtained by means of a
Baldwin, Lima & Hamilton Strain Indicator (Fig. 5). For a
power-screw torque of 37 in-lbf a maximum axial force of 241
lbf may be obtained. Of course, the stress in the specimen
will be a function of its cross sectional area.

Temperature control, or heating, is obtained by embedded
Watlow Heaters [Ref. 13] in the left cross head and the load
cell arm. Temperature is controlled by a 0-120 VAC variac
input to the heaters and is measured by copper-constantan
T/C's mounted under each hold-down (Figure 5). Cooling from
temperatures greater than ambient is obtained by thermal
conduction and radiation within the vacuum chamber.

The reinforced phenol-formaldehyde bucket thermally in-
sulates the strain/heating stage assembly from the remainder
of the microanalysis stage there by minimizing its increase
in temperature, and possible thermal distortion of the SEM's
internal components.

IV. DESIGN DETAILS

A. PRELIMINARY COMMENTS

In order to meet the limitations and specifications, as
established in section II, several questions had to be an-
swered prior to the design of specific components.

First, what materials are to be used? Because of its
relatively high strength (σ_{yt} = 40 K_{psi}) [Ref. 8], non-magne-
tic properties and availability, 304 stainless steel was se-
lected as the load carrying structural material. Reinforced
phenol-formaldehyde was selected as an insulator because of
its lower thermal conductivity ($4 \times 10^{-4} \frac{cal\ cm}{cm^2\ sec°C}$) [Ref. 12]
non-magnetic properties, reasonable strength and availability.

Second, how is the heat to be applied and measured? Since
specimens are observed in a vacuum environment resulting in
little or no heat loss due to convection, it was decided to
use thermal conduction for heat application. The commercially
available Watlow Firerod Cartridge Heater was selected as the
heat source. Justification for this selection is evident from
its specifications (see Figure 6). The most simple and
compatable of temperature measurement systems was utilized,
the type T (copper-constantan) thermocouple.

Third, how is the stress/strain to be applied? Obviously
size is of major concern, therefore because of its simplicity,
ease of fabrication, and compactness, parallel crossheads

22

WATLOW

1/8" FIREROD® CARTRIDGE HEATER

Only the Watlow FIREROD ⅛" cartridge heater can give you the high wattage, high temperature, long life capabilities for applications where it is essential to minimize size.

* Swaged construction for maximum life and efficiency.
* Up to 100 watts/in.² (40 watts per linear inch) at 1400°F.
* Up to 400 watts/in.² (160 watts per linear inch) at 1000°F.
* Corrosion resistant incoloy or inconel sheath.
* Heated lengths from ¾" to 11-½".

DIMENSIONAL DATA

TYPE I- Externally connected leads

.122" ± .002"   #24 solid nickel pins   #24 AGT flexible nickel or nickel plated wire

¼" Unheated   ¼" Unheated   1-½"   Insulated sleeves

1-¼" to 12" ±3% Overall length   10" standard
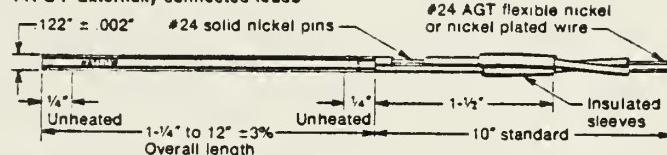
TYPE II- Internally connected leads

.122" ± .002"   #24 AGT flexible nickel or nickel plated wire

¼" Unheated   ½" Unheated   10" Standard

1-½" to 12" ±3% Overall length
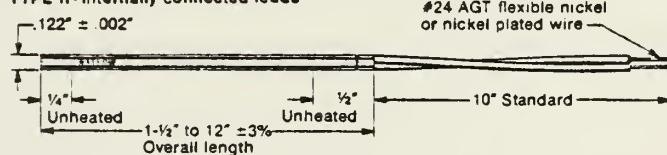
MATERIALS & CONSTRUCTION

SHEATH - Incoloy and Inconel are used for their excellent resistance to corrosion and oxidation at high temperatures.

END DISC - The standard end disc is swaged in place. A welded end disc is available when requested.

RESISTANCE WINDING - Nickel-chromium wire, helically wound and equidistant to the sheath at all points for even heat distribution.

INSULATION - The winding is insulated from the sheath with magnesium oxide, compacted by swaging for maximum heat transfer and dielectric strength.

TEFLON SEAL - An optional Teflon seal at the leads protects against moisture. A welded end disc and Teflon-insulated lead wires are included. Temperature at the seal must not exceed 275°F. An unheated length of 1" or more is recommended.

EXTRA UNHEATED LENGTH - Provided as requested.

ELECTRICAL DATA

AMPS - Maximum = 3 amps.

VOLTS - 12 to 250 volts.

WATTS - Minimum = 8 watts at 120VAC, 32 watts at 240VAC. Use the graph below to determine the maximum allowable for your application. Tolerance = +5%−10%.

OHMS - 45 to 2000 ohms per inch of heated length. Tolerance = +10%−5%.

Fit in hole (inches)

Maximum watts per inch of heated length
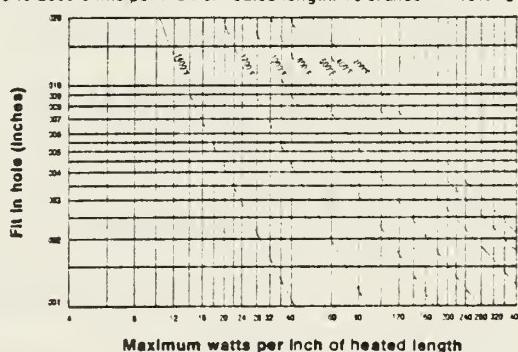
Figure 6.   Watlow firerod specifications

23

driven by opposed power-screw pairs are employed. This arrange-
ment also favors the measurement of the applied load and the
application of heat, as well as linear readout of specimen
elongation.

Fourth, how is the input torque to be applied and trans-
mitted to the power-screw? When the microanalysis stage is
stripped, the θZ and $\theta Z'$ control knobs are not employed. As
these two controls are equipped with a linear digital readout,
they present an appropriate torque input system. Unfortunately,
the θZ and $\theta Z'$ extensions lay normal to the power-screws. To
alleviate this situation and gain elongation sensitivity, a
worm and worm gear assembly is called for.

B. WORM AND WORM GEAR

Initial investigations revealed that the machine shops at
the Naval Postgraduate School were capable of manufacturing
a worm but not a worm gear of less than one inch in diameter.
In view of time limitations and expense of having the assembly
fabricated by an outside contractor, it was decided that the
worm and worm gear be procured ready made. An in depth re-
view of available gear catalogs was fruitful in that the
Boston Gear Division of North American Rockwell lists and
stocks a highly desirable 48 pitch worm and worm gear assembly.
See Figures 7 and 8 respectively.

The fact that the worm is steel and not bronze or 304 SS
was alarming but once purchased, the machine shop could

duplicate it in SS if necessary. Therefore, two complete
assemblies were purchased. (worm # GLSH and worm gear # G1018,
Refs. 6 and 7 respectively).

C. CROSS-HEADS

The cross-head design was the most logical starting place
because the minimum length of a cross-head is set by the maxi-
mum length of the Watlow Firerod, which is to be embedded
within, and the worm gear clearance requirements. From Figure
7 it may be seen that the minimum length is 1.25" for a 1/8"
diameter firerod. The firerod diameter also sets the minimum
width of the cross-head, which was taken to be 1/4", making
it possible to fabricate the cross-heads from 1/4" 304 SS
plate.

To maintain vertical alignment upon application of torque
to the power-screws, vertical alignment tabs were incorporated
into each end of the cross-head. These tabs fit tightly in
grooves machined into the bucket ends (to be discussed later).

To accomodate the power-screws and worm gear clearance,
the left cross-head was drilled and tapped 1/4-20 UNC-LH and
the right cross-head was drilled and tapped 1/4-20 UNC-RH.
In addition, the right cross-head was truncated in height to
permit attachement of the load cell. The left cross-head was
drilled and tapped to accept a hold-down (see Figure 4).

48 PITCH
SINGLE THREAD

LEAD = .0654″
LEAD ANGLE = 3° 35′

HLSH worm has threads polished but not ground. GLSH worm has threads ground and polished. All worms have No. 47 (.0785) drilled hole in hub for driving pin.

ORDER BY CATALOG NUMBER

Cat. No.		List Price		Pitch	Face	Hole	Hub	
Soft	Hard	Soft	Hard	Diam.			Diam.	Proj.
LSH	HLSH	$2.58	$4.22	.333″	³⁄₁₆″	⁵⁄₁₆″	.26″	³⁄₁₆″
...	GLSH	...	5.95	.333	³⁄₁₆	⁵⁄₁₆	.26	³⁄₁₆

† To tips of teeth.

Figure 7. Worm specifications

WORM GEARS—BRONZE

Stocked right-hand only.

14½° PRESSURE ANGLE

48 PITCH
SINGLE THREAD
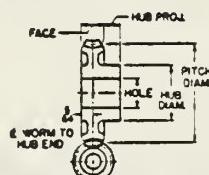
5/32″ FACE
RATIO = TEETH ÷ 1

ORDER BY CATALOG NUMBER

Cat. No.	List Price	Teeth	Pitch Diam.	Hole	Hub Diam.	Hub Proj.	O.D.†	Style
G1018	$2.79	20	.417″	3/16″	11/32″	3/16″	.48″	Plain
G1019	3.70	30	.625	3/16	7/16	1/4	.69	"
G1020	4.41	40	.833	3/16	1/2	1/4	.89	"
G1021	5.51	50	1.042	3/16	1/2	1/4	1.10	"
G1024	6.18	60	1.250	3/16	5/8	1/4	1.31	"
G1022	7.31	80	1.667	1/4	5/8	5/16	1.73	"
G1023	9.88	100	2.083	1/4	11/16	5/16	2.14	Web

Figure 8. Worm gear specifications

D. POWER-SCREW

Once the worm gears were selected, the power-screw could
be designed. The worm gear hole diameter is 3/16". This
establishes the minimum power-screw diameter. 3/16" is also
very close to the minor diameter for a 1/4-20 UNC thread.
Therefore it was then decided to use 1/4-20 UNC -RH and LH
threads on the power-screw.

If the maximum axial force was to be induced into a spe-
cimen then the input torque (T_{TR}) requirement to each power-
screw had to be established. The calculations for T_{TR}
follows:

   Calculation 1: torque required to raise 50 lbf load w/o
                   off-set.

$$T_{TR} \atop {50\,lbf} \quad = \quad \frac{F\,d_m}{2}\left(\frac{l + \pi\,\mu\,d_m}{\pi\,d_m - \mu\,l}\;\frac{sec\;\alpha}{sec\;\alpha}\right) \qquad \text{[Ref. 10]}$$

From Ref. 9 (for a 1/4-20 UNC screw)

   d = 0.2500 in

   N = 20

   A_t = 0.0318 in²

   A_r = 0.0269 in²

from Ref. 1 (for metal-to-metal)

   μ = 0.3

$$\alpha = ARCTAN\left(\frac{\frac{P}{2}}{\frac{d - d_r}{2}}\right) \qquad \text{[Ref. 10]}$$

28

where $\qquad d_c = \sqrt{\dfrac{4 A_c}{\pi}} = 0.1851 \text{ in}$

$$P = \ell = \frac{1}{N}$$

and $\qquad d_m = \dfrac{d + d_c}{2} = 0.2175 \text{ in}$

solving for α:

$$\alpha = \text{ARCTAN}\left(\frac{\frac{1}{(2)(20)}}{\frac{0.2500 - 0.1851}{2}}\right) = 37.6°$$

now solving for T_{TR}:

$$T_{TR}_{50 \text{ lbf}} = \frac{(50)(0.2175)}{2}\left(\frac{0.05 + (\pi)(0.3)(0.2175)\left(\frac{1}{\cos 37.6}\right)}{(\pi)(0.2175) - (0.3)(0.05)\left(\frac{1}{\cos 37.6}\right)}\right) = \underline{2.53 \text{ in} \cdot \text{lbf}}_{\text{power-screw}}$$

[Note: The full 50 lbf load was used in the above calculation
    because in one crosshead each power-screw carries one
    half the load (25 lbf) but there are two cross-heads
    per power-screw.]

Calculation 2: Torque required to separate cross-heads because
        of additional frictional forces imposed due
        to 50 lbf load being off-set from center line
        of power-screw axis. (Note: This is a very
        rough approximation.)

For worst case or maximum T_{TR} from Figures 9 and 10 let:
  off-set

$F = 25 \, lbf$ $\qquad\qquad$ $d_1 = d = 0.2500 \, in$

$\ell_1 = 0.25 \, in$ $\qquad\qquad$ $\mu = 0.3$

$\ell_2 = 0.6875 \, in$ $\qquad\qquad$ $r = \dfrac{d}{2}$

The couple $F_1 - F_1$ must balance the moment caused by the force

off-set or:
$$F\ell_2 = F_1 \ell_1$$

solving for $\overline{F}_1$:
$$F_1 = \frac{F \ell_2}{\ell_1}$$

from Figure 10 it may be shown that:
$$T_{TR}_{\text{OFF-SET}} = 2\mu F_1 r = \mu F_1 d$$

substituting for $\overline{F}_1$:

$$T_{TR}_{\text{OFF-SET}} = \frac{\mu F \ell_2}{\ell_1} \quad (d)$$

$$= \frac{(0.3)(25)(0.6875)}{0.25} \quad (0.2500)$$

$$= 5.16 \, in \cdot lbf$$

Thus, the torque required for each power-screw due to the

loading off-set is $2 \, T_{TR}_{\text{off-set}}$, since figure 10 only considers

off-set

30
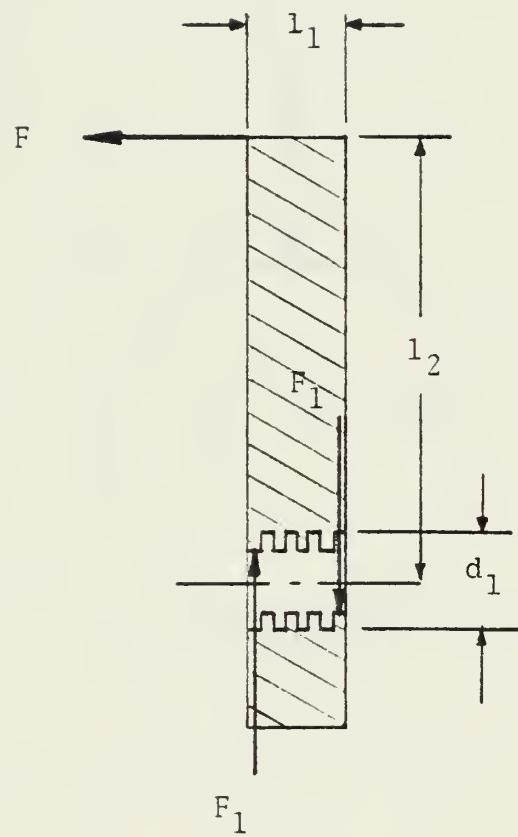
Figure 9. Cross-head force diagram
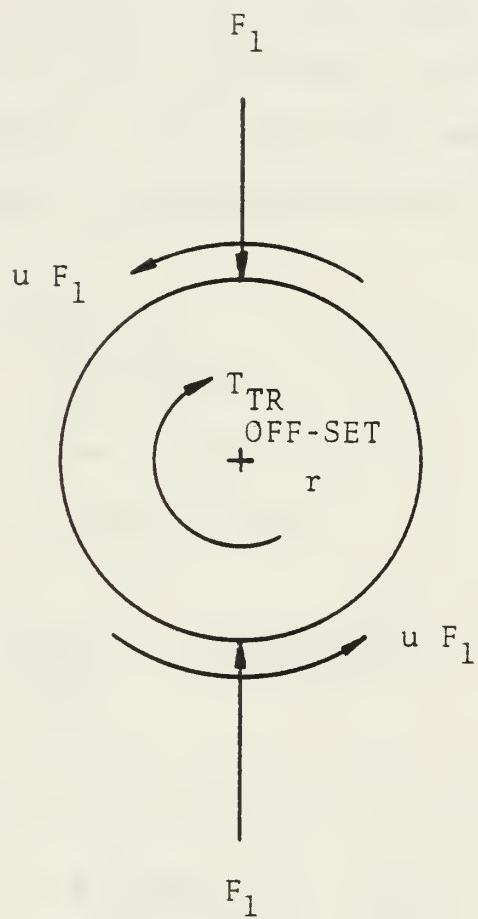
Figure 10. Power-screw force diagram

one cross-head penetration. The summation of calculations 1
and 2 defines the total torque input required per power-screw
at full load and is;

$$T_{TR_{TOTAL}} = T_{TR_{50\,lbf}} + 2\,T_{TR_{off\text{-}set}} = 10.27 \; \frac{in \cdot lbf}{power \cdot screw}$$

If one assumes a uniform shaft of diameter dr with applied
moments of 17.19 in-lbf (1/2 maximum load times off-set) and a
length of 1 inch (maximum cross-head separation plus 2 times
the half thickness of one cross-head), then the maximum bend-
ing moment, shear force, end slopes and deflection may be
calculated. By means of superposition and Figure 11, calcu-
lations are as follows:

From Ref. 6 for 304 SS:

$$\sigma_{uts} = 82.4 \; Kpsi$$

$$\sigma_{yt} = 40 \quad Kpsi$$

$$E = 28 \times 10^6 \; psi$$

From Figure 11,

$$I = \frac{\pi d^4}{64} = \frac{(\pi)(0.25)^4}{64} = 1.92 \times 10^{-4} \; in^4$$

The maximum deflection occurs at $x = \frac{1}{2} = 0.5$ in. and is:

$$\delta_{max} = 2\left(\frac{MLx}{6EI}\right)\left(1 - \frac{x^2}{L^2}\right)$$

$$= \frac{(2)(17.19)(1)(0.5)}{(6)(28\times10^6)(1.92\times10^{-4})}\left(1 - \frac{(0.5)^2}{(1)^2}\right)$$

$$= 4.00 \times 10^{-4} \; in$$
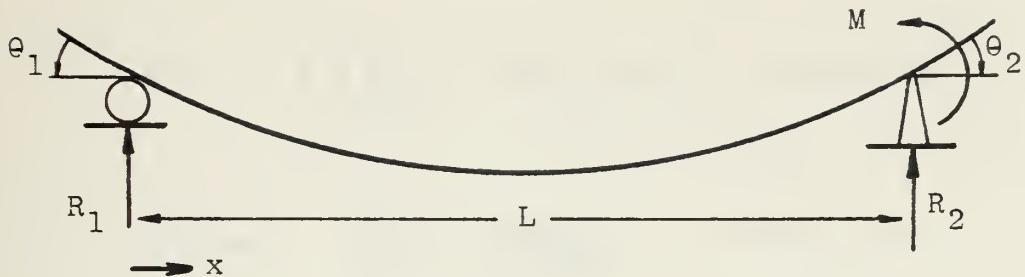
REACTIONS: $R_1 = R_2 = \frac{M}{L}$

DEFLECTIONS AT ANY POINT x :

$$\delta = \frac{MLx}{6EI}\left(1 - \frac{x^2}{L^2}\right)$$

SLOPES : $\theta_1 = \frac{ML}{6EI}$; $\theta_2 = \frac{ML}{3EI}$

MAXIMUM SHEAR FORCE AT ALL x:

$$F_S = \frac{M}{L}$$

Where I for a circular section is:

$$I = \frac{\pi d^4}{64}$$

Figure 11. Free body diagram of simple supported beam

The maximum shear stress $\left(\gamma_{BENDING}\right)$ occurs at all x:

$$F_s = 2\left(\frac{M}{L}\right) = (2)\left(\frac{17.19}{1}\right) = 34.38 \text{ lbf}$$

$$\gamma_{BENDING} = \frac{F_s}{A_s} = \frac{34.38}{0.0269} = 1278.1 \text{ psi}$$

The maximum end slopes $\left(\Theta_1 \text{ and } \Theta_2\right)$ are identical.

$$\Theta_1 = \Theta_2 = \frac{ML}{6EI} + \frac{ML}{3EI} = \frac{ML}{2EI}$$

$$= \frac{(17.19)(1)}{(2)(28 \times 10^6)(1.92 \times 10^{-4})}$$

$$= 1.60 \times 10^{-3} \text{ in/in}$$

and
$$\text{Tan } \Theta = \frac{\Theta_1}{1} = \Theta_2$$

so that
$$\Theta = 9.17 \times 10^{-2} \text{ DEGREES}$$

Therefore the maximum deflection of each cross-head at the point of maximum axial force loading (50 lbf) is expressed as:

$$\partial_{CROSS-HEAD} = \ell_2 \cos\left(90 - \Theta\right)$$

$$= (0.6875)\cos\left(90 - 9.17 \times 10^{-2}\right) = 1.10 \times 10^{-3} \frac{\text{in}}{\text{CROSS-HEAD}}$$

More usefully stated, at full load the maximum error in cross-head separation read out due to bending in the power-screws will be 2∂ cross-head or 2.20×10^{-3} in and should be deducted

35

from the original readout for elongation. Because this value is sufficiently large, if specimens are of maximum gage length and a maximum axial loading of approximately 50 lbf is expected, the digital readout for elongation should be corrected for the power-screw bending.

The bending stress ($\tau_{BENDING} = 1278.1 \ psi$) in the power-screws is small when compared to the ultimate stress ($\sigma_{ULTS} = 82.4 \ kpsi$), the tensile yield stress ($\sigma_{YT} = 40 \ kpsi$) and the shear yield stress ($\sigma_{YS} = 20 \ kpsi$) for 304 SS. This being the situation, and because the rotation rate of the power-screws is so slow, shaft rotational fatigue calculations were not performed. However, the combined effects of bending and torsion were investigated as follows:

From Ref. 9:

$$\tau_{TORSION} = \frac{T r}{J}$$

where T = torque input to power-screws between cross-heads.

$$= 6.43 \ in\text{-}lbf$$

$$r = \frac{d}{2} = \frac{0.1851}{2} = 0.0925 \ in$$

and
$$J = \frac{\pi \, d_r^4}{32} = \frac{(\pi)(0.0925)^4}{32} = 7.20 \times 10^{-6} \ in^4$$

solving for $\tau_{TORSION}$:

$$\tau_{TORSION} = \frac{(6.43)(0.0925)}{(7.20 \times 10^{-6})} = 82.6 \times 10^3 \ psi$$

combining torsional and bending shear stress:

36

$$\tau_{MAX} = \tau_{TORSION} + \tau_{BENDING}$$

$$= 82.6 \times 10^3 + 1278.1 = 83.9 \times 10^3 \text{ psi}$$

Giving a factor of safety (n) of

$$n = \frac{\sigma_{ye}}{2\tau_{max}} = \frac{40 \times 10^3}{(2)(83.9 \times 10^3)} = 0.24$$

utilizing the maximum shear stress theory.

The arrived at factor of safety is obviously quite low, but not surprising. The assumptions made for the approxima-tion of T_{TR} off-set are as follows:

1)   u = 0.3 for metal-to-metal;

2)   maximum gage length (o.5 in)

and 3)   maximum specimen axial force (50 lbf).

Though not formally presented herein, it can be shown that for a worst case situation, the stress induced by thermal expansion of the power-screws upon heating a specimen is less than two percent of the stress induced by straining a shape-memory effect alloy and then heating it through its reversion tempera-ture. It is also noteable that the thermally induced stress caused by expansion of the power-screws and the reduction of stress caused by bending of the power-screws , tend to nullify one another.

E. LOAD CELL

The load cell is similar to the simply supported beam shown in Fig. 12, where F is the maximum strain induced force in a specimen. The load cell is fastened to the right cross-head by means of two 5-44 UHF 304 SS socket head screws. Strain measurements are made by temperature compensating strain gages whose output is measured by means of a strain indicator.

In order to properly select and procure an appropriate strain gage, the strain produced in the load cell was calculated as follows:

Assumption: Uniform, simply supported beam (Figure 11). Because of its lower modulus of elasticity, 7075- T651 aluminum was selected as the material for fabrication of the load cell.

From Ref. 11 for 7075- T651 aluminum alloy

$$\sigma_{ues} = 78.0 \ k \, psi \qquad\qquad \sigma_{\gamma t} = 67.0 \ k \, psi$$

$$E = 10 \times 10^{6} \ psi$$

Recalling basic statics and referring to Figure 12,

$$\sigma = \frac{Mc}{I}$$

where

$$M = \frac{F\ell}{2} = \frac{(50)(1.125)}{2} = 28.13 \ in \cdot \ell bf$$

$$c = h/2 = 0.125/2 = 0.0625 \ in$$

and by superposition,

$$I = \frac{bh^{3}}{12} - \frac{b'h^{3}}{12} = \frac{h^{3}}{12}(b - b')$$
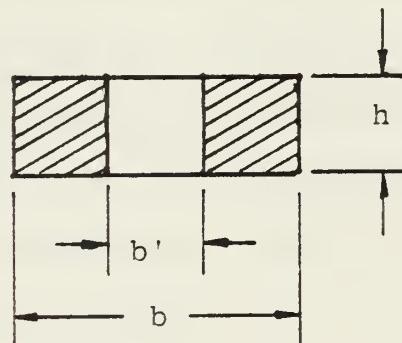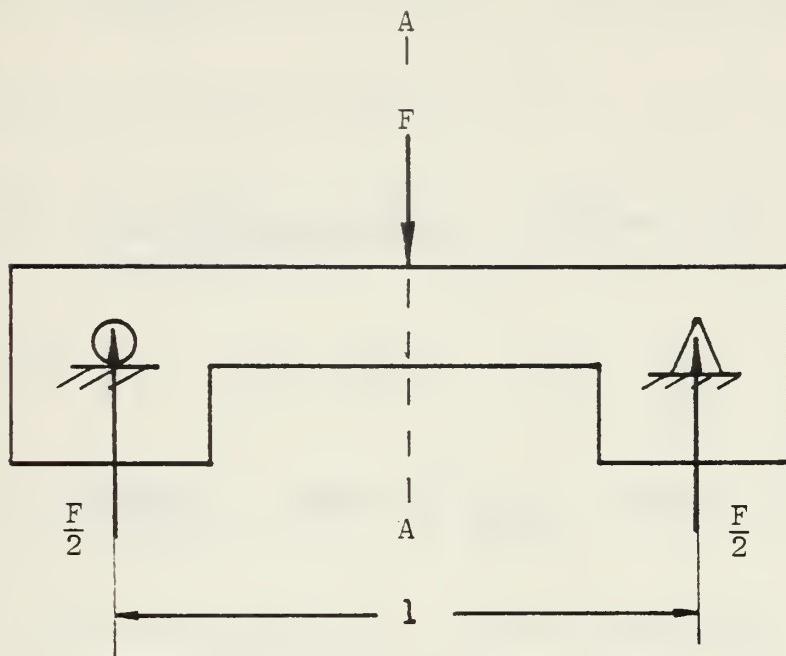
Section A-A end on view.

From drawing B-5,

$$h = 0.125"$$
$$b = 0.5"$$
$$b' = 0.125"$$
$$l = 1.125"$$

Figure 12. Free body diagram of load cell

$$I = \frac{(0.125)^3}{12}(0.5 - 0.125) = 6.10 \times 10^{-9} \text{ in}^4$$

substituting and solving for σ:

$$\sigma = \frac{(28.125)(0.0625)}{(6.10 \times 10^{-5})} = 28800 \text{ psi}$$

but $\quad \sigma \equiv E\epsilon \quad$ so that $\quad \epsilon = \frac{\sigma}{E}$

thus $\quad \epsilon = \frac{28800}{10 \times 10^6} = 2.88 \times 10^{-3} \frac{\text{in}}{\text{in}} = 2880 \text{ micro } \frac{\text{in}}{\text{in}}$

With this calculation for ϵ having been made, an appropriate strain gage may be selected. From Ref. 6, the smallest strain gage that is available with leads and that has a sensitivity range encompassing the calculated ϵ, is the PI -00 - 030 CG - 120 - L. This gage was subsequently ordered. However, it was not readily available so the supplier recommended and provided an acceptable substitute. The PI -00 - 031 CG - 120 - L which is only slightly larger.

F. LOAD CELL ARM

Returning to components fabricated of 304 SS, the load cell arm is configured in such a manner so as to accommodate an embedded firerod, secure a hold-down and permit mid-beam loading of the load cell. A roll pin fastens the load cell arm to the load cell. This is the location of maximum stresses which are in the form of shear and crushing.

40
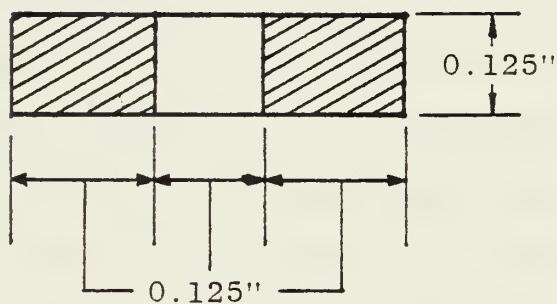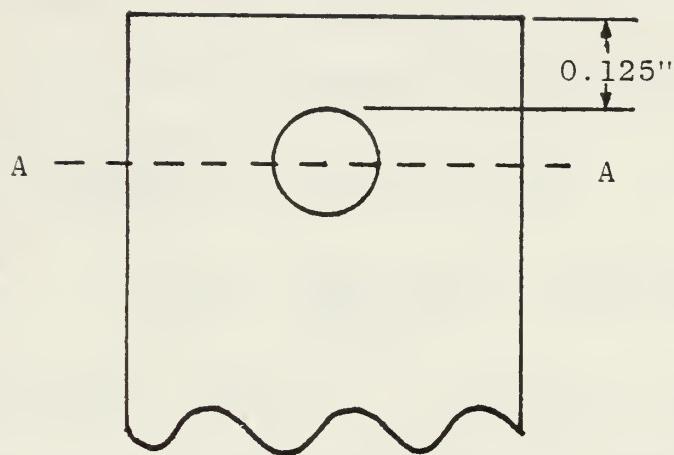
Figure 13. Load cell arm stress area

From Figure 13 for compressive loading,

$$A_b = \left(\frac{1}{8}\right)\left(\frac{1}{8}\right) = 1.56 \times 10^{-2} \; in^2$$

so that $\qquad \sigma_{BEARING} = \dfrac{F}{A_b} = \dfrac{50}{1.56 \times 10^{-2}} = 3200 \; psi$

Which is much less than the maximum crushing yield stress of
40 Kpsi. For shear loading,

$$A_s = 2\left(\frac{1}{8}\right)\left(\frac{1}{8}\right) = 3.13 \times 10^{-2} \; in^2$$

so that $\qquad \sigma_s = \dfrac{F}{A_s} = \dfrac{50}{3.13 \times 10^{-2}} = 1600 \; psi$

Here gain, $\sigma_s << \sigma_{YS} = 20 \; Kpsi$. Therefore, there is no
fear of failure in the load cell arm due to shear or crushing.

G. HOLD-DOWN

The hold-down is nothing more than a flat section of 304
SS with two drill holes in it. It's function is to securely
fasten each end of the specimen to its respective cross-head
by means of two 5-44 UNF 304 SS sochet head screws. For a
maximum force of 50 lbf, the hold-down must exert the follow-
ing normal force (Fn) to each end of a specimen:
As may be observed in Fig. 14, if a force balance is performed,

$$\bar{F} = 2 \mu \bar{F}_n$$

so that $\qquad \bar{F}_n = \dfrac{\bar{F}}{2\mu}$

where $\qquad \mu = 0.6 \qquad$ for rough metal-to-metal surfaces
$\qquad\qquad\qquad\qquad$ [Ref.1]

42
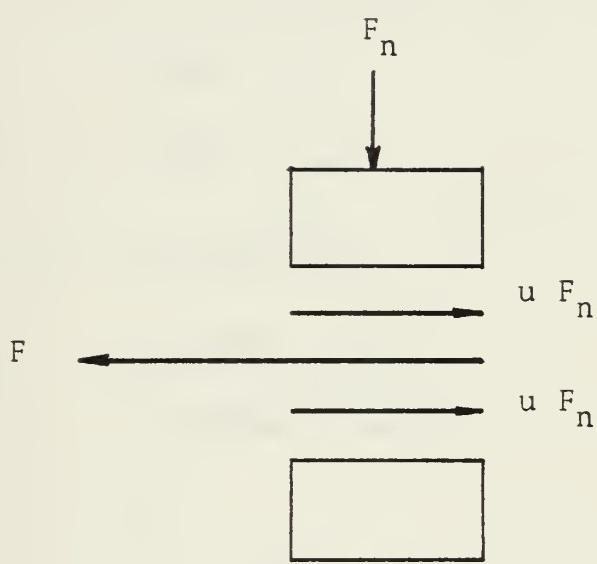
Figure 14. Free body diagram of hold-down

solving: $F_n = \dfrac{50}{(2)(0.6)} = 41.7$ lbf

The force is the minimum which must be applied by the torquing of the two 5-44 UNF sochet head SS screws. The minimum screw torque requirement was established as shown.

$$T = \frac{F_n d_m}{2}\left(\frac{l + \pi \mu d_m \sec \alpha}{\pi d_m - \mu l \sec \alpha}\right) + \frac{F_n \mu d_c}{2} \qquad \text{[Ref. 10]}$$

From Ref. 3, for a 5-44 UNF socket head screw

$$d_c = 0.2050 \text{ in}$$

$$d = 0.1250 \text{ in}$$

From Ref. 9 for the same screw,

$$A_t = 0.00880 \text{ in}^2$$

$$A_r = 0.00716 \text{ in}^2$$

$$N = 44$$

and as before, $\mu = 0.3$

Recalling similar power-screw calculations,

$$d_r = \sqrt{\frac{4 A_r}{\pi}} = \sqrt{\frac{(4)(0.00716)}{\pi}} = 0.0955 \text{ in}$$

$$P = \frac{1}{N} = l$$

$$d_m = \frac{d + d_r}{2} = \frac{0.125 + 0.0955}{2} = 0.1102 \text{ in}$$

44

$$\alpha = \text{ARCTAN}\left(\frac{\frac{P}{2}}{\frac{d-d_r}{2}}\right)$$

$$= \text{ARCTAN}\left(\frac{\frac{1}{(2)(44)}}{\frac{0.1250-0.0955}{2}}\right) = 37.61°$$

Substituting and solving for T,

$$T = \frac{(41.7)(0.1102)}{2}\left(\frac{(0.0227)+(\pi)(0.3)(0.1102)\left(\frac{1}{\cos 37.61}\right)}{(\pi)(0.1102)-(0.3)(0.0227)\left(\frac{1}{\cos 37.61}\right)}\right)$$

$$+ \frac{(41.7)(0.3)(0.2050)}{2}$$

$= 2.33 \text{ in} \cdot \ell bf$, a value which may easily be applied
by means of tightening with a standard Allen wrench of appro-
priate size.

H. BUCKET ASSEMBLY

The entire bucket assembly was fabricated of reinforced
phenol-formaldehyde (trade name bakelite). Since the sole
purpose of the bucket assembly is to insulate and support the
power-screws, and because no forces of any consequence are
transmitted to the bucket assembly, stress calculations were
not performed. The assembly was designed however, to main-
tain zero axial motion of the power-screws and prevent

vertical movement of the cross-heads. This was accomplished
by hand finishing and fitting of the power-screws, cross-heads
and bucket assembly. Additionally the maximum dimensions of
the bucket assembly are in keeping with the stereoscan limita-
tions as established earlier.

I. WORM SHAFT

Before the design of the worm shaft or shaft support
could be accomplished, the forces associated with worm and
worm gear had to be determined. For the selected worm and
worm gear assembly, Ref. 7 provides the following specifications:

$$N = 20$$

$$d_G = 0.417 \text{ in}$$

$$P_n = 48$$

$$\phi_n = 14\tfrac{1}{2}°$$

Lead = 0.0654 in

$$\lambda = 3° 35' \doteq 3.583°$$

Referring to Figure 15,

$$W^X = W \cos \phi_n \sin \lambda$$

$$W^y = W \sin \phi_n$$

$$W^z = W \cos \phi_n \cos \lambda$$

For a full load axial force of 50 lbf in a specimen, it was
determined than an input torque of 7.69 in-lbf was required
per power-screw. The force (W), required to provide this
torque, acts through the pitch diameter of the worm gear, so
W is determined as shown:
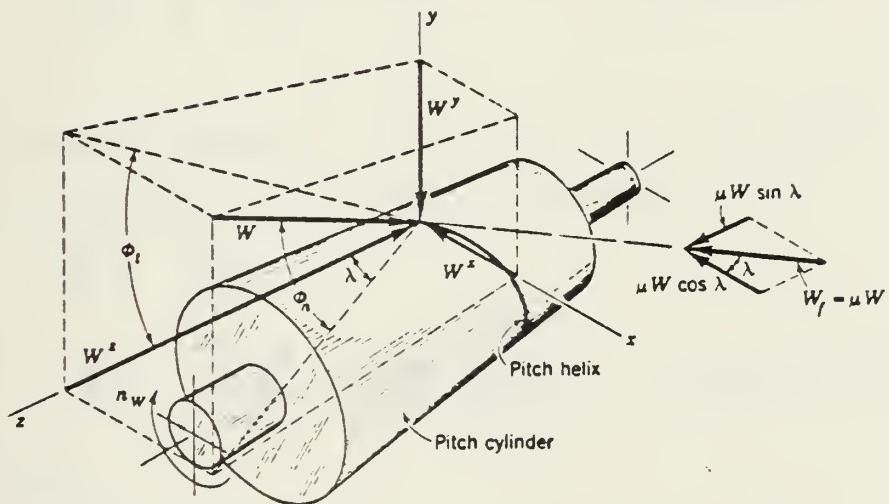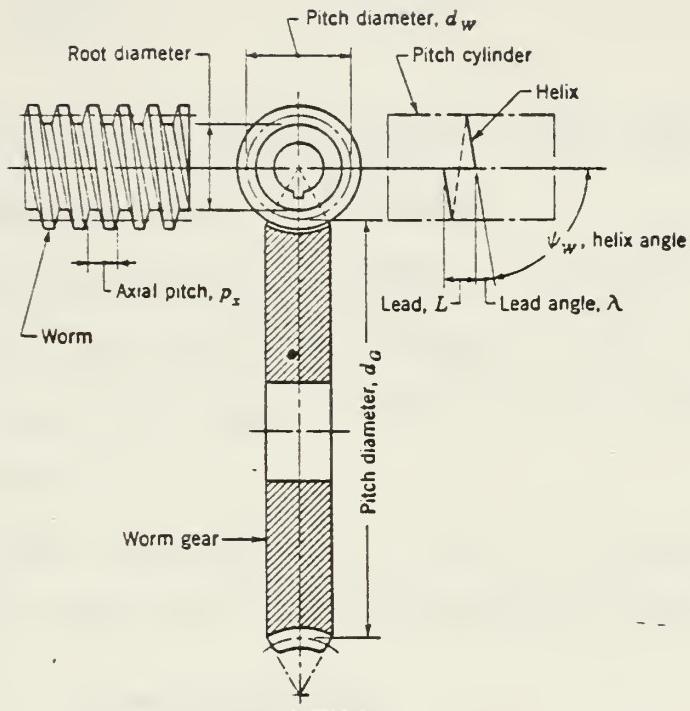
Figure 15.   Worm and Worm Gear Nomenclature

$$T_{TR} = \frac{W d_G}{2}$$
Total

or $W = \dfrac{2\, T_{TR}}{d_G}^{Total} = \dfrac{(2)(7.69)}{0.417} = 36.88 \; lbf$

Thus,

$$W^X = (36.88)(\cos 14.5)(\sin 3.583) = 2.23 \; lbf$$

$$W^Y = (36.88)(\sin 14.5) = 9.23 \; lbf$$

and $W^Z = (36.88)(\cos 14.5)(\cos 3.583) = 9.22 \; lbf$

These quantities also verify the assumption that the forces
acting on the bucket are small indeed and the neglection of
same is justified.

The worm shaft, constructed of 304 SS is supported hori-
zontally at both ends, thus the maximum shear force is deter-
mined as:

$$F_s = \sqrt{(W^x)^2 + (W^Y)^2} = 9.50 \; lbf$$

The worm shaft diameter is set by the worm hole which is 3/16"
[Ref. 6], leading to the calculation of σ_s,

$$\sigma_s = \frac{F_s}{A_s}$$

where

$$A_s = \frac{\pi d^2}{4} = \frac{(\pi)\left(\frac{3}{16}\right)^2}{4} = 0.0276 \; in^2$$

Substituting:

$$\sigma_s = \frac{9.50}{0.0276} = 344.1 \; psi$$

So that:

$$n = \frac{20 \times 10^3}{344.1} = 58.1$$

48

Leading to the conclusion that the shaft is definitely of safe design. Like calculations for the shear stresses in the power-screw at its bucket support would also yield approximately the same results.

The final consideration on the design of the worm shaft was that of coupling it to the θZ ($\theta Z'$) extension. The θZ ($\theta Z'$) extensions are equipped with universal joint couplings thus it was decided to utilize these couplings. One end of the worm shaft was machined such that its outside diameter was equal to the inside diameter of the universal joint (1/8 inch by direct measurement).

The original design called for the worms to be pinned to the worm shaft but due to an over tolerance situation after machining, the worms were pressed on to the worm shaft.

J.   SHAFT SUPPORT

The shaft support was designed to fulfill these require-ments:

(1)   Allow for alignment of worm and worm gear;

(2)   Minimize axial and transaxial motion of the worm shaft. For alignment purposes it was decided to have a single compo-nent shaft support rather than a separate support for each end of the worm shaft. The single unit support was constructed of 304 SS and the worm shaft journals were line bored.

The shaft support is secured to the bucket assembly by two 5-44 UNF SS socket head screws extending through elongated

holes which facilitate alignment of the worm and worm gear assemblies.

The shaft support has two major stress areas, one located at the worm shaft journal and the other at the screw fasteners (Figure 16). These points are subject to shear stresses and were evaluated.

From the discussion on the worm shaft it maybe shown that the shear forces at the journal are:

$$F_s = \sqrt{(W^Y)^2 + (2W^Z)^2} = 20.62 \text{ lbf}$$

(Note: W^Z is doubled as there are two worm gear assemblies whose W^Z acts only on one journal shear area at a time and depends on the direction of worm rotation.)

From Figure 16, at the shaft journal

$$A_s = \left(\frac{1}{16}\right)\left(\frac{3}{16}\right) = 0.0820 \text{ in}^2$$

so that
$$\sigma_s = \frac{F_s}{A_s} = \frac{20.62}{0.0820} = 251.5 \text{ psi}$$

and
$$n = \frac{\sigma_{ys}}{\sigma_s} = \frac{20 \times 10^3}{251.5} = 79.5$$

Again from Figure 16, the two socket head screw fasteners are a limiting design point, and must be considered.

$$A_s = A_{\bullet} = 0.00716 \text{ in}^2$$

and
$$F_s = \sqrt{(W^Y)^2 + (W^Z)^2} = 13.05 \text{ lbf}$$

F_s F_s

$A_r = 0.00716''$

SOCKET HEAD
SCREWS

F

JOURNAL

$\frac{7}{16}''$

$\frac{3}{16}''$
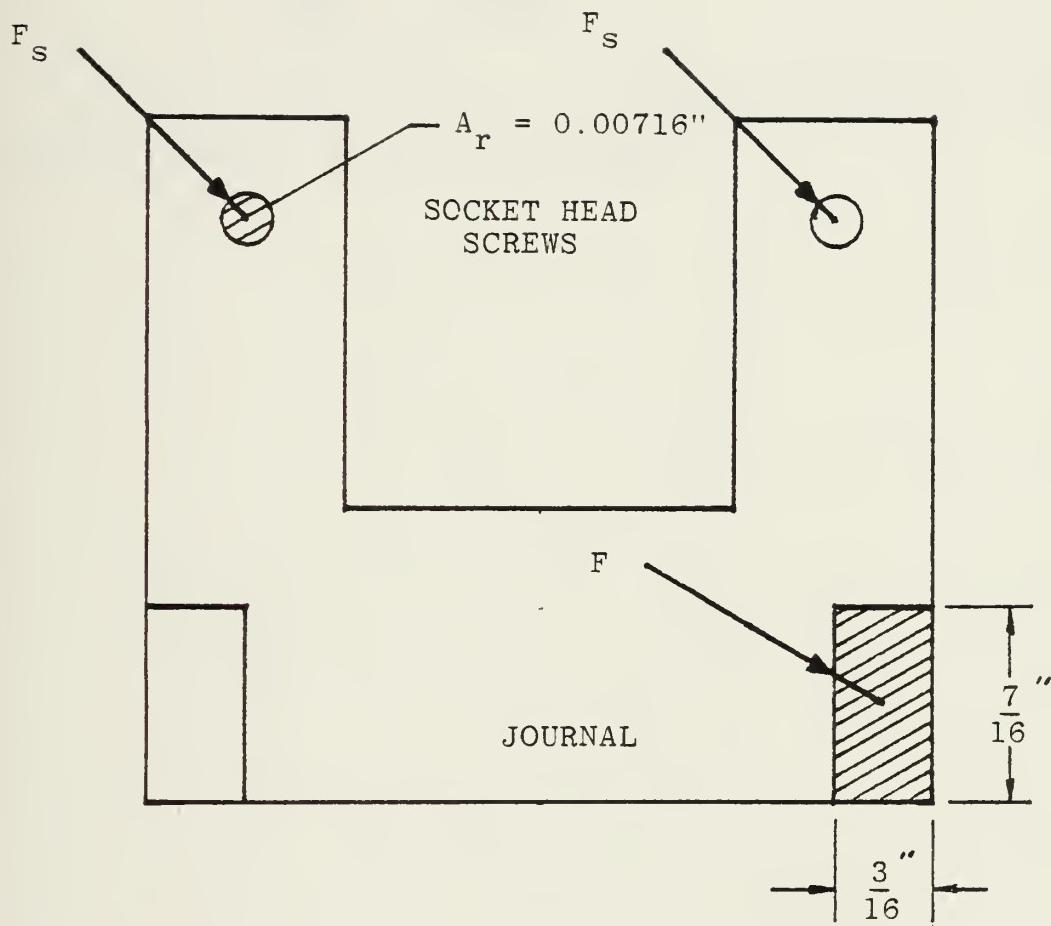
Figure 16. Shaft support stress areas

51

Since the two screws share the shear load. Solving for σ_s,

$$\sigma_s = \frac{\bar{F}_s}{A_r} = \frac{13.05}{0.00716} = 1822.6 \text{ psi}$$

Thus

$$n = \frac{\sigma_{ys}}{\sigma_s} = \frac{20 \times 10^3}{1822.6} = 11.0$$

As seen several times before, n is high and therefore, fear of material failure is very low indeed.

V. TESTS AND CALIBRATION

A. WATLOW FIREROD

The two firerods are embedded in components of different masses therefore it was decided to supply power to the fire-rods by attaching each one to it's own 0-120 VAC variac unit. Data was collected in the following manner:

(1)   Thermocouples were fastened under each hold-down.

(2)   A thermocouple was fastened to a mounted specimen.

(3)   The microanalysis stage was placed in the SEM.

(4)   The SEM was placed in operation.

(5)   Voltage to the right cross-head firerod was increased by increments of 2 VAC starting at 0 VAC.

(6)   After each 2 VAC increment the voltage of the left cross-head firerod was increased gradually.

(7)   At each voltage level sufficient time was allowed for equilibrium temperature to be attained.

(8)   VAC right, VAC left, millivolts T/C right, millivolts T/C left and millivolts T/C specimen were recorded.

(9)   At the end of the run (room temperature to 120°C) each T/C was evaluated using a boiling water reference. The data collected is listed in Appendix A. The same data appears graphically in Figure 17.
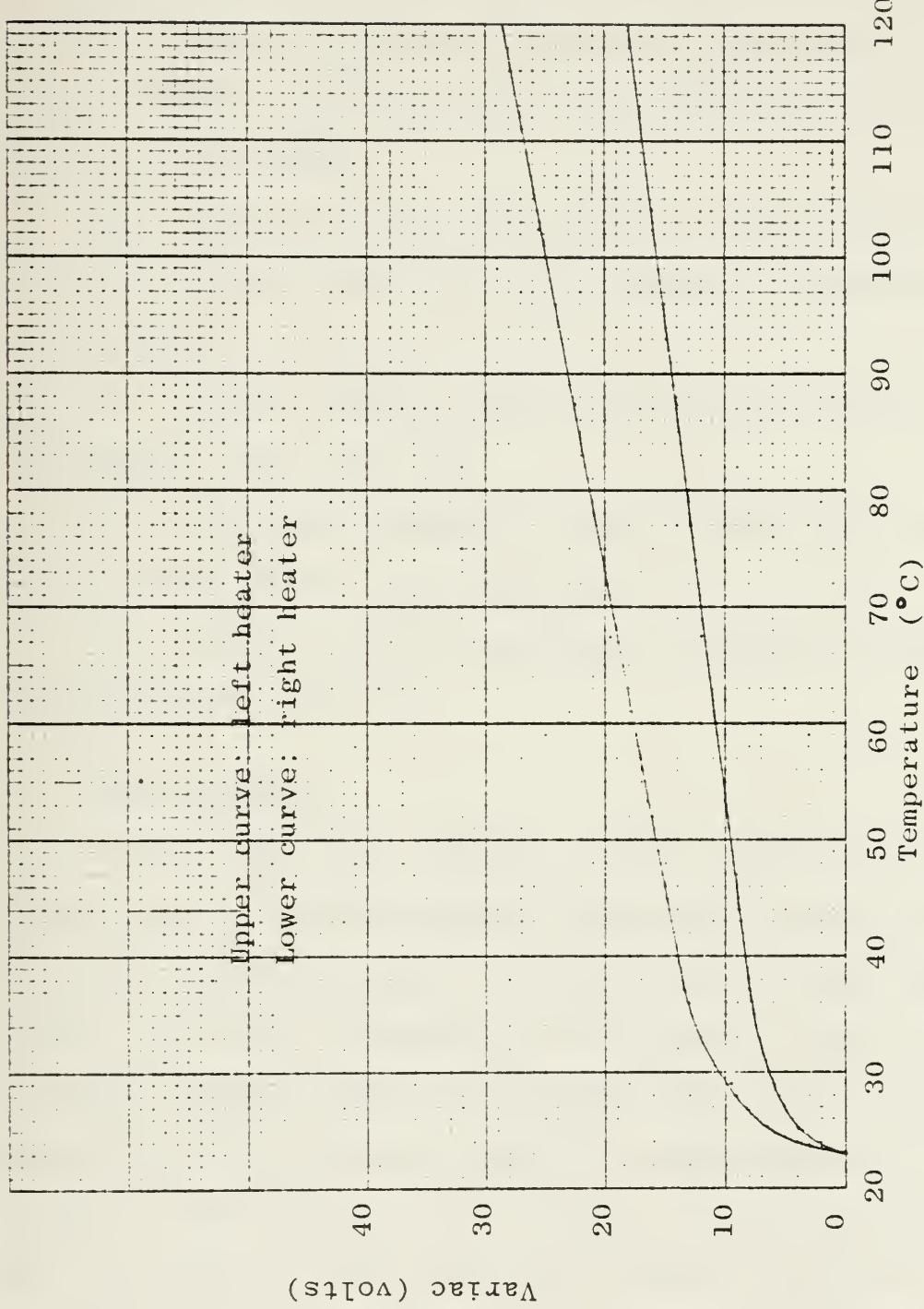
Figure 17. Temperature response curves

54

B. LOAD CELL

Due to the late arrival of the ordered strain gages, they had not been installed or evaluated at the time of this writing. However, the dead weight calibration procedure outlined below is prescribed.

(1) Detach the load cell from the right cross-head.

(2) Suspend the load cell by means of the elongated screw holes.

(3) Suspend weights from the load cell arm in 5 lbf increments, from 0-50 lbf.

(4) Utilizing a Baldwin, Lima and Himilton strain indicator record data at each increment.

(5) Reduce data and plot curve for strain indicator reading versus load (F).

C. STAGE ASSEMBLY

To test the stage assembly, it was initially decided to video tape the strain enduced formation of martensite and its reversion (upon heating) of a brass family shaped-memory-effect alloy, which will be referred to as Alloy E. With the aid of a unique cutting tool, the specimens were cut to length (3/4 inch) and the well known tensile specimen dumb-bell shape was formed. After shaping, the specimens were electro-polished for 5 seconds in a 10% potassium cyanide solution @ 15 VAC, followed by a 4 second etch in a solution consisting of 2.5 grams $Fe\ Cl_3$, 25 milliliters of 37% HCl and 25 milliliters of H_2O.

A specimen was then mounted in the strain/heating stage such that the gage length was 0.25 in.

The initial angle of tilt on the stage was zero. In later tests this angle was increased to 15° from the horizontal position. The effect was to improve SEM resolution by increasing the contrast of surface relief.

Following normal SEM operating procedures, the specimen was observed in the normal mode and then transferred to the TV mode. Here it was observed that focusing and resolution were very poor on powers greater than 2000x, even with aperture 3 and the upper two condensing lenses open as wide as possible. Resolution was much improved when minor adjustments to center the filament were made. The test was started by engaging the video tape machine.

While most of the grains of Alloy E were martensitic, there were some grains which were reltaively free of martensite. By use of the X and Y positioning controls an area was selected for observation, one with little martensite.

With the magnification set at 2000x, a discontinuous strain rate was applied. An elongation increase of 0.0004 in. was applied every 10 seconds to a maximum of 0.0128 in. (5% strain), since martensite should form when strained. A replay of the video tape and observation by several researchers proved fruitless; no apparent microstructural changes were detected.

On the belief that the microstructural changes were not within the filed of view, several other Alloy E specimens were prepared with a variety of stress concentration configurations. Observation of these specimens under tensile loading revealed more of the same, nothing, except for a discoloration of the specimens surface where it had been exposed to the electron beam at 5000x.

On the chance that "nothing" was an acceptable observation, another specimen was prepared. This specimen was a 70-30 brass specimen, annealed at 575°C for 1.5 hours and furnace cooled. Its dimensions were 0.75 X 0.25 X 0.003 in. without the dumb-bell shape but with a very small hole punched in the center of the specimen as a stress concentrator.

The specimen was electro-polished for 50 seconds in a 10% potassium cyanide solution at 20 VAC, and then etched as Alloy E had been. The stage tilt angle was set at 15° from the horizontal and as before the specimen was made ready for video taping..

A location between the punch mark and the closest edge was selected for observation. This time the magnification was set at 1000x to allow for the larger gain size and view a larger area.

Upon elongation of the 0.25 inch gage length to 0.2772 in. the formation of slip bands were observed and videotaped, thus demonstrating the strain capabilities of the stage.

The results obtained with the annealed brass specimen left an unresolved observation associated with Alloy E as it had been monitored under like stress conditions. It was then decided to observe another brass family shape-memory-effect alloy, Alloy B.

Alloy B is 100% martensite at room temperature since its Ms temperature is approximately 50°C. It also has a reversion temperature of approximately 70°C. If heated to a temperature greater than 70°C the martensitic reversion should be observable.

Alloy B specimens were prepared as were the Alloy E specimens. After mounting, a specimen was made ready for the video recording of its reversion process. Voltages corresponding to a 120°C equilibrium temperature were set on the variacs and taping began. Once again, no discernable microstructural changes were noticed. Several more Alloy B specimens were prepared, mounted, heated through the reversion temperature, cooled through Ms and recorded, with the same results as before, including the discoloration of the area under observation.

Suspecting that the specimen may not be attaining the temperatures as indicated by continuous T/C readings, the T/C's were once more checked against a boiling water reference with satisfactory results. A T/C was also mounted to a specimen appropriately secured on the stage. This check showed that the specimen temperature w/o the electron beam on was within ±0.5°C of the temperature monitored at the hold-downs.

Therefore, the Alloy B specimen should have attained the temperatures recorded during the observation period.

VI. DISCUSSION AND CONCLUSIONS

The video recordings of the annealed brass specimens clearly demonstrate that the stage will strain specimens as specified. The calibration data indicates that the firerods are capable of heating specimens to at least 120°C. The lack of observed microstructural changes anticipated in the shape-memory Alloys B and E still remains a mystery.

While it is beyond the scope of this thesis to investigate further and explain the results obtained with the shape-memory-effect alloys, the following are offered as possible explanations:

(1) First and most obvious, the microstructural changes are not occurring within the field of view.

(2) The strain rates are low and there is no rapid change in specimen temperature, therefore the driving forces for the resultant microstructural changes are low, thus the surface relief changes associated with microstructural changes are so slow that they cannot be detected at normal play back speeds.

(3) The specimen is subjected to a 200 micro AMP, 20 KV electron beam, resulting in I^2R heating.
Since Ms and the reversion temperature are reasonably low, there is a possibility that the local temperature of the specimen, under the electron beam and that which is being recorded, is greater than the reversion temperature. If this were the

situation, then indeed one would observe no microstructural changes. The observable darkening in contract of the shape-memory-effect alloys may also tend to support this theory.

The low factor of safety determined in the combined bending and torsional shear stress analysis is not of major concern for two reasons. First, the other major stage components are over designed so that a shearing of the power-screws between the cross-heads and gear is a desirable failure mode and location as there will be no resultant damage to any other strain/heating stage component or to the SEM. Second, during initial testing, some axial forces induced were determined to have exceeded 50 lbf and no determinantal effects were observed. This suggests that the design assumptions are very convective, particularly the assumed coefficient of friction in the power-screws.

A recommended improvement to the strain/heating stage is the reorientation of the power-screws such that the specimen and the power-screws are in the same geometric plane. This would eliminate the large shearing stress associated with the torque required to raise the 50 lbf off-set load.

In conclusion, the strain/heating stage, while not of optimum design, appears to operate as desired. The strain gages remain to be installed and the load cell calibrated. Lastly, further investigation and experimentation needs to be conducted in connection with the shape-memory-effect alloys

in order to establish the exact reason or reasons for no readily observable microstructural changes upon straining, heating and or cooling.

APPENDIX: A

FIREROD CALIBRATION DATA

RIGHT VARIAC (VAC)	RIGHT T/C (mV)	RIGHT TEMP (°C)	LEFT VARIAC (VAC)	LEFT T/C (mV)	LEFT TEMP (°C)	AVAC (VAC)
0	0.908	23	0	0.908	23	0
2	0.935	23.7	3	0.935	23.7	1
4	1.00	25.3	6.5	1.00	25.3	2.5
6	1.155	29.0	9.6	1.155	29.0	3.5
8	1.490	37.1	13.5	1.490	37.1	5.5
10	2.140	53.4	16.5	2.140	53.4	6.5
12	2.80	67.6	19.5	2.80	67.6	7.5
14	3.695	87.4	22.5	3.695	87.4	8.5
16	4.39	102.4	25.5	4.39	102.4	9.5
18	5.21	119.6	28.5	5.21	119.6	10.5

SPECIMEN T/C (mV)	SPECIMEN TEMP (°C)
0.905	22.9
0.934	23.6
0.995	25.1
1.15	28.9
1.495	37.2
2.135	52.3
2.80	67.6
3.685	87.2
4.375	102.1
5.20	119.4

Data was reduced for °C by
linear interpolation of
data published in Ref. 5.

EQUIPMENT:

Simpson I70 Ser. # M885
Leeds and Northrup Millivolt Potentiometer Ser. # 1577585
General Radio Co. Variac Ser. #M979
Superior Electric Co. Powerstat Ser. #None
T/C Copper-Constantan

APPENDIX: B

DRAWINGS OF STAGE COMPONENTS
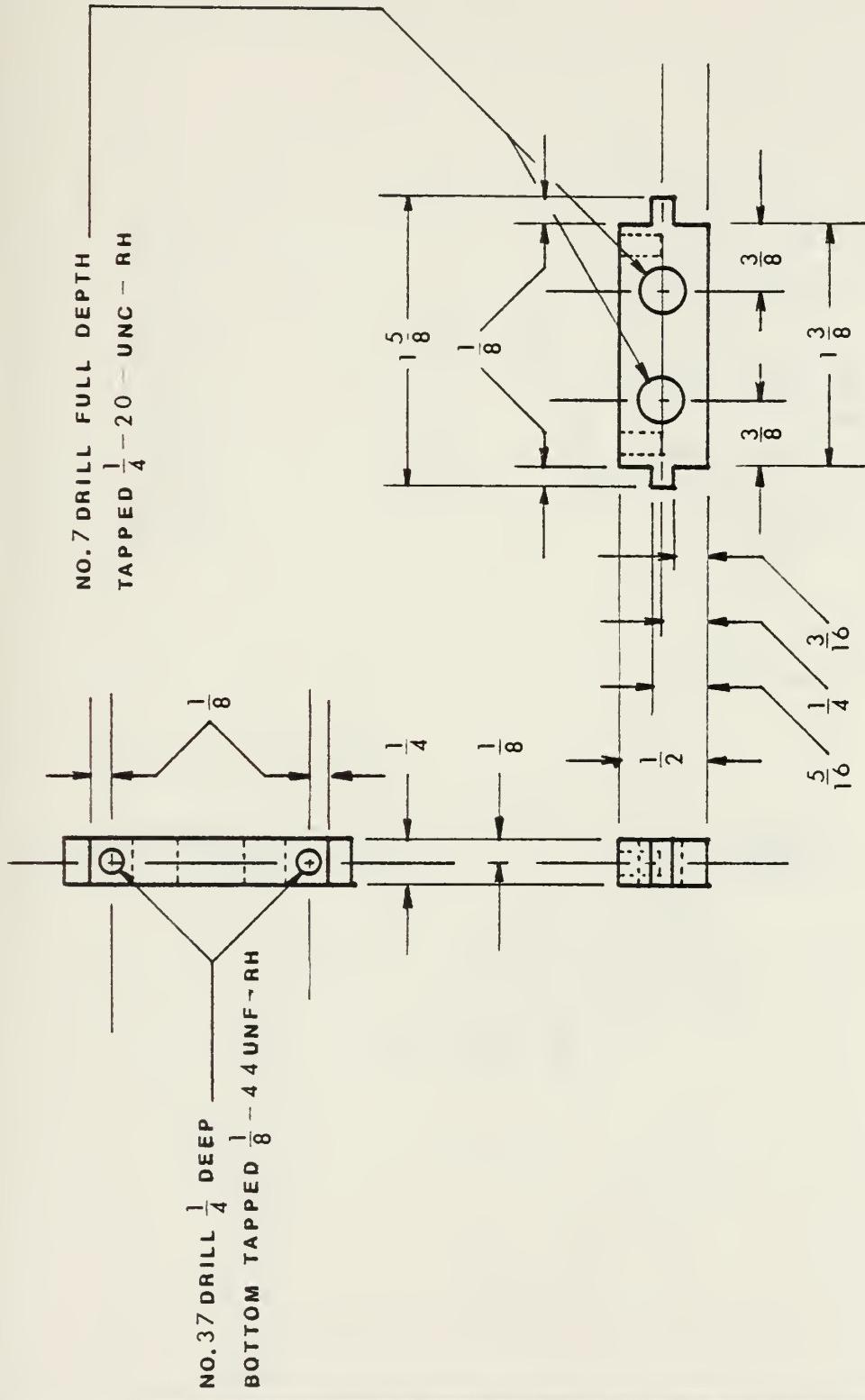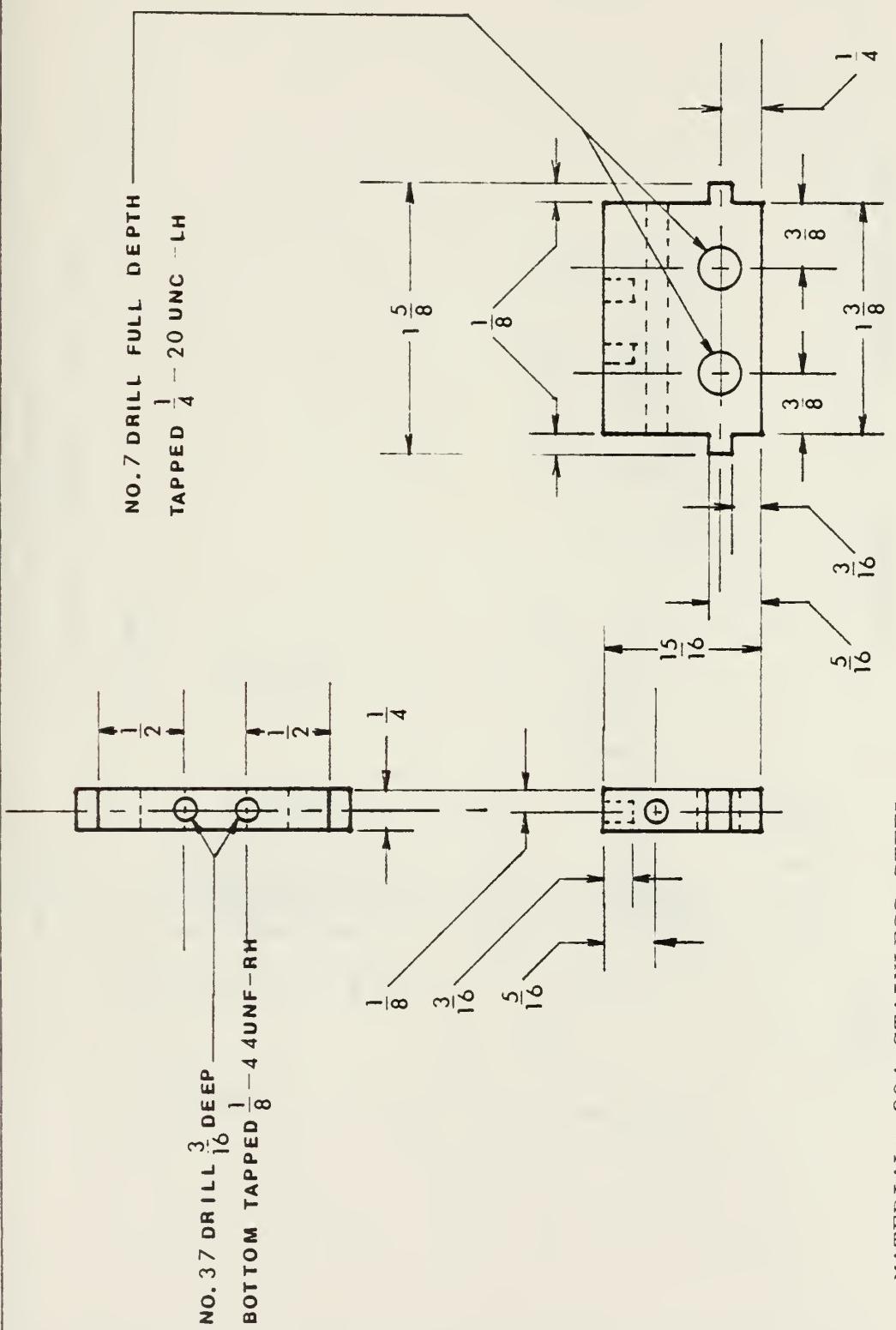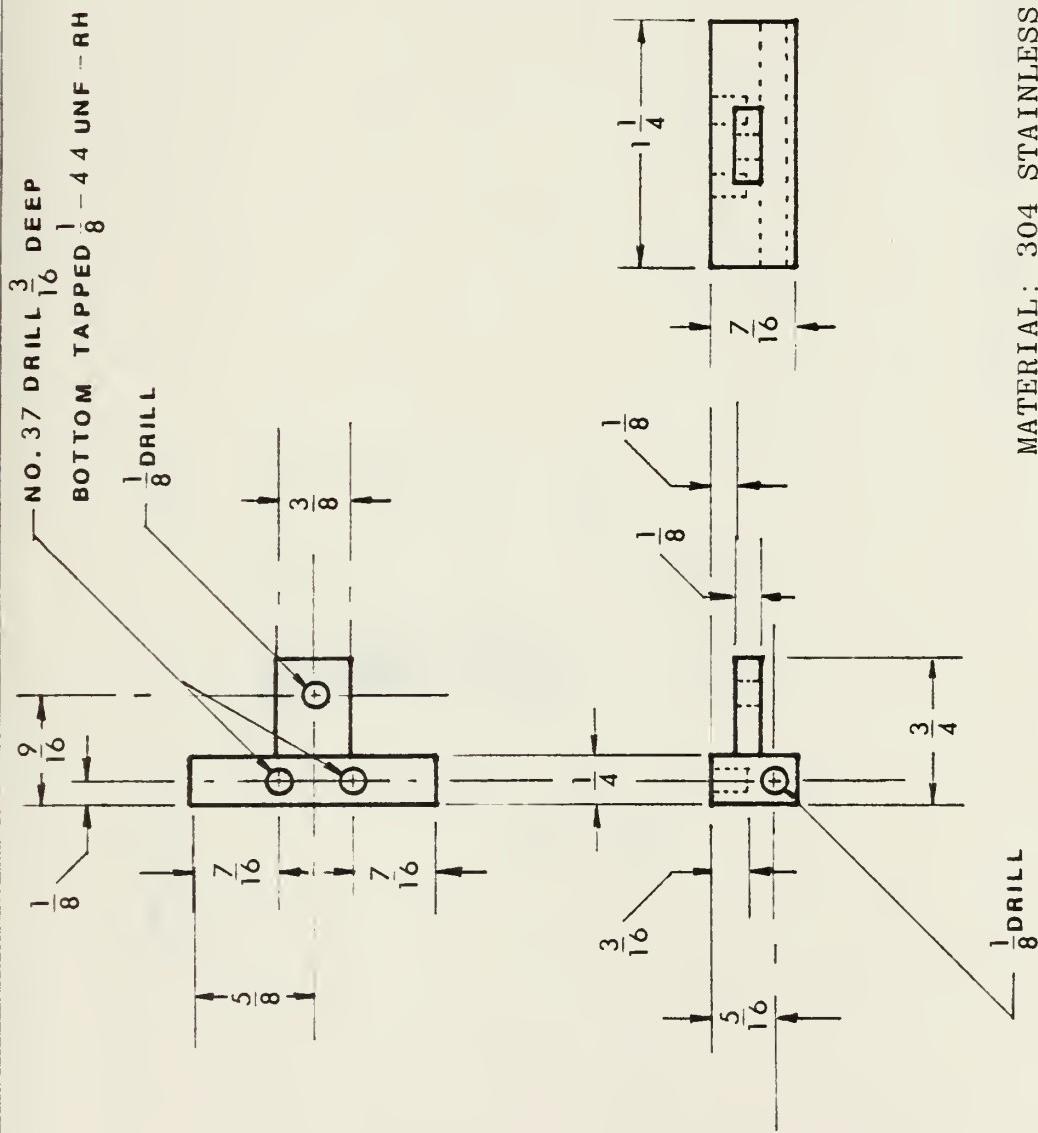
64

NO. 7 DRILL FULL DEPTH

TAPPED $\frac{1}{4}$ – 20 – UNC – RH

NO. 37 DRILL $\frac{1}{4}$ DEEP

BOTTOM TAPPED $\frac{1}{8}$ – 44 UNF – RH

MATERIAL: 304 STAINLESS STEEL

| RIGHT CROSS HEAD | R. CAMPBELL | SCALE: $"= 1"$ | B-1 |

65

NO.7 DRILL FULL DEPTH

TAPPED $\frac{1}{4}$ - 20 UNC - LH

$1\frac{5}{8}$

$\frac{1}{8}$

$\frac{3}{8}$

$\frac{3}{8}$

$1\frac{3}{8}$

$\frac{3}{8}$

$\frac{1}{4}$

$\frac{3}{16}$

$\frac{15}{16}$

$\frac{5}{16}$

$\frac{1}{2}$

$\frac{1}{2}$

$\frac{1}{4}$

NO. 37 DRILL $\frac{3}{16}$ DEEP

BOTTOM TAPPED $\frac{1}{8}$ - 4 4UNF - RH

$\frac{1}{8}$

$\frac{3}{16}$

$\frac{5}{16}$

MATERIAL: 304 STAINLESS STEEL

| LEFT CROSS HEAD | R.CAMPBELL | SCALE: 1" = 1" | B-2 |

66

NO. 37 DRILL $\frac{3}{16}$ DEEP

BOTTOM TAPPED $\frac{1}{8}$ – 44 UNF – RH

$\frac{1}{8}$ DRILL

$\frac{9}{16}$

$\frac{3}{8}$

$\frac{1}{8}$

$\frac{7}{16}$

$\frac{7}{16}$

$\frac{1}{8}$

$\frac{5}{8}$

$\frac{1}{4}$

$\frac{3}{4}$

$\frac{3}{16}$

$\frac{5}{16}$

$\frac{1}{8}$ DRILL

$\frac{1}{4}$

$\frac{7}{16}$

MATERIAL: 304 STAINLESS STEEL

| LOAD CELL ARM | R. CAMPBELL | SCALE: 1" = 1" | B-3 |

67

MATERIAL: 304 STAINLESS STEEL

$\frac{3}{16}$

$\frac{3}{4}$

$\frac{1}{4}$

$\frac{1}{16}$

$\frac{3}{16}$

$\frac{1}{8}$

$\frac{1}{8}$ DRILL

| HOLD-DOWN | R. CAMPBELL | SCALE: 1″ = 1″ | B-4 |

68

NO.30 DRILL FULL DEPTH

$\frac{1}{8}$

$\frac{1}{8}$

$\frac{1}{4}$

$\frac{1}{2}$

$\frac{1}{8}$

$\frac{1}{4}$

$1\frac{3}{8}$

$\frac{1}{2}$

$\frac{1}{2}$

MATERIAL: 7075–T651 ALUMINUM ALLOY

| LOAD CELL | R.CAMPBELL | SCALE: $1'' = 1''$ | B–5 |

NO.37 DRILL FULL DEPTH
TAPPED $\frac{1}{8}$ – 44UNF – RH
REMAINING 4 HOLES NO.30 DRILL
FULL DEPTH

MATERIAL: BAKELITE

| BASE SIDE | R. CAMPBELL | SCALE:1" = 1" | B-6 |

70
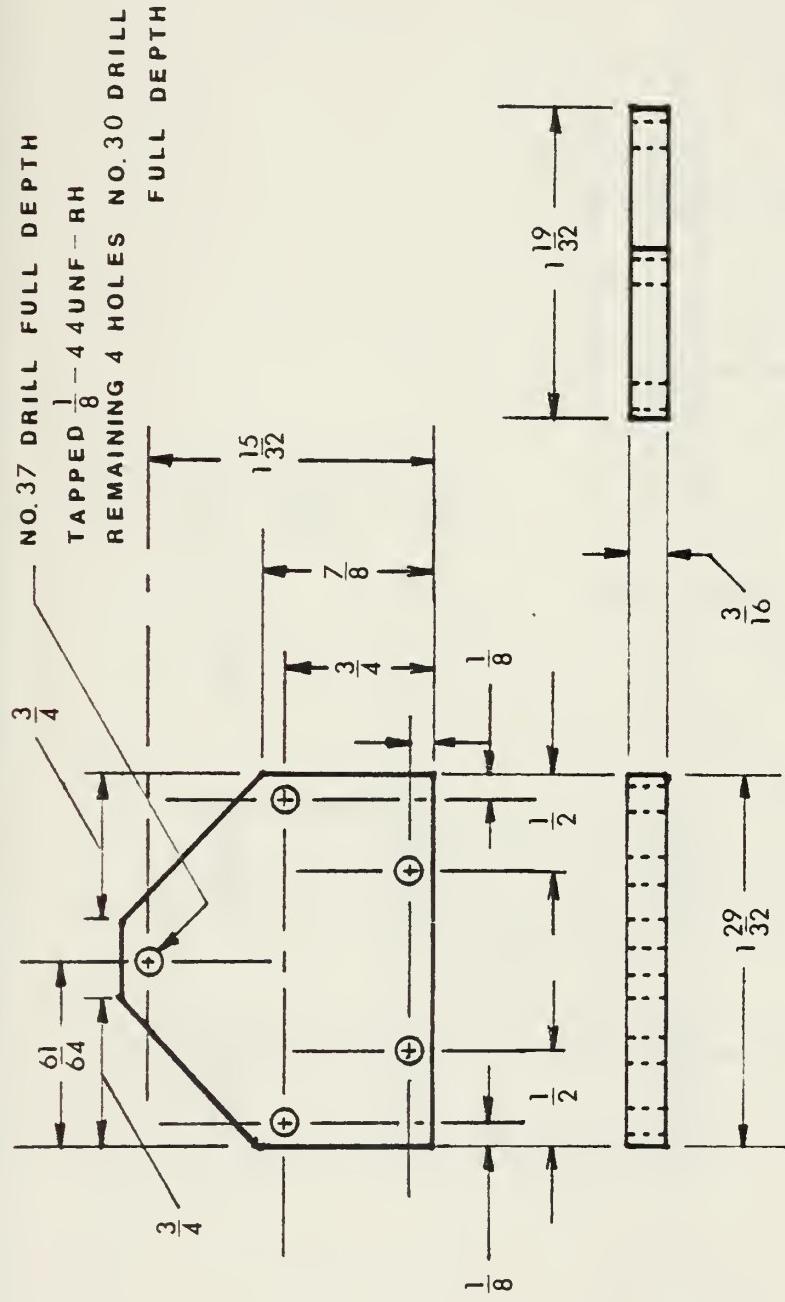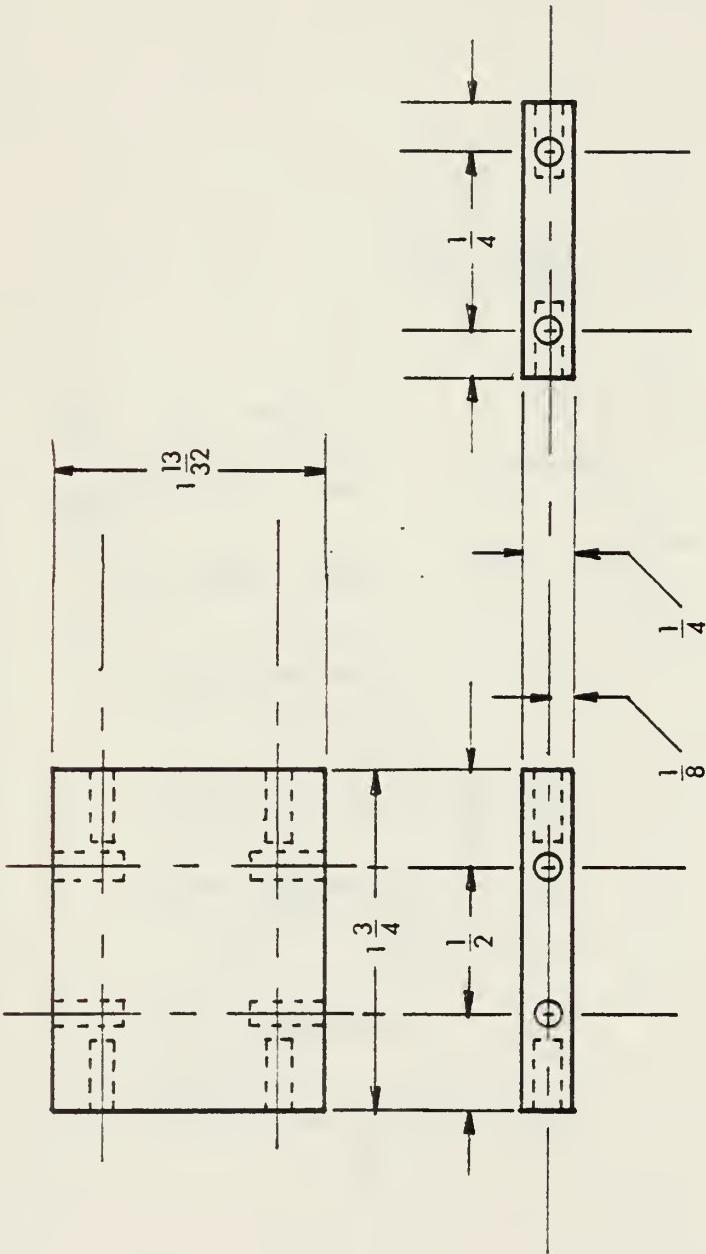
8 HOLES NO. 37 DRILL $\frac{3}{8}$ DEEP TAPPED $\frac{1}{8}$ — 44 UNF — RH

MATERIAL: BAKELITE

| BUCKET BASE | R.CAMPBELL | SCALE: 1"=1" | B-7 |

71

NO. 30 DRILL FULL DEPTH

$\frac{1}{8}$

$\frac{15}{32}$

$\frac{19}{32}$

$\frac{7}{8}$

$\frac{1}{2}$

$1\frac{3}{4}$

$\frac{1}{8}$

$\frac{1}{4}$

$\frac{1}{8}$
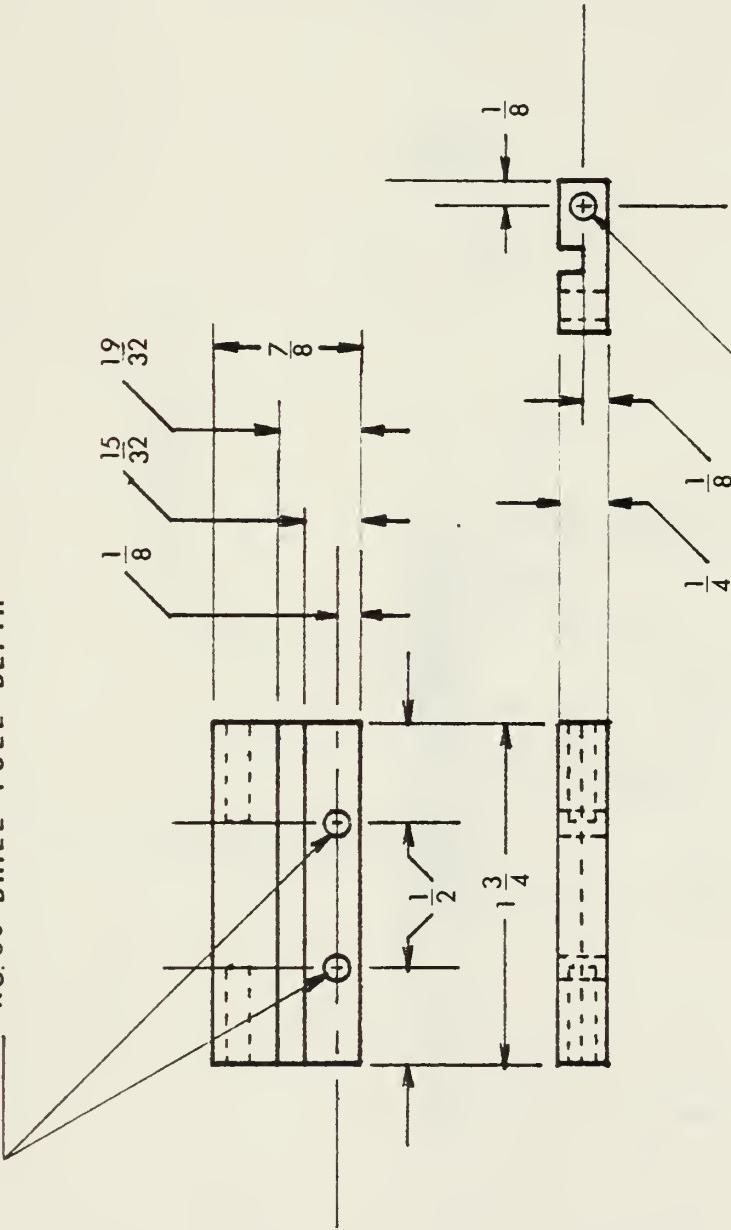
2 HOLES NO. 37 DRILL $\frac{1}{2}$ DEEP
TAPPED $\frac{1}{8}$ — 44 UNF — RH

MATERIAL: BAKELITE

| BUCKET FACE | R.CAMPBELL | SCALE: 1" = 1" | B-8 |

73
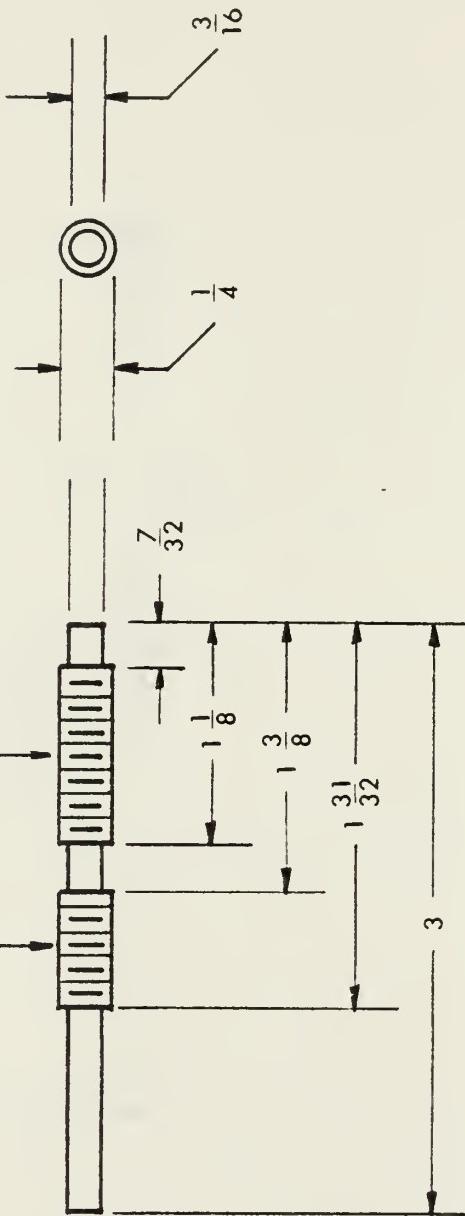
POWER SCREW   R. CAMPBELL   SCALE: 1"=1"   B-9

MATERIAL: 304 STAINLESS STEEL

$\frac{1}{4}$-20 UNC - LH

$\frac{1}{4}$-20 UNC - RH

$\frac{3}{16}$

$\frac{1}{4}$

$\frac{7}{32}$

$1\frac{1}{8}$

$1\frac{3}{8}$

$1\frac{31}{32}$

3
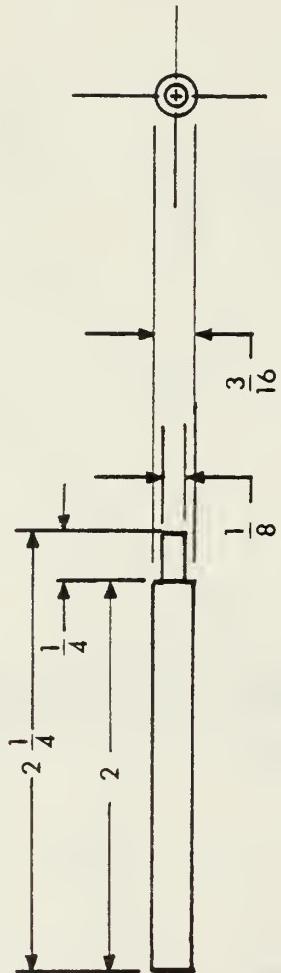
MATERIAL: 304 STAINLESS STEEL

| WORM SHAFT | R. CAMPBELL | SCALE: 1" = 1" | B-10 |

MATERIAL: 304 STAINLESS STEEL

NO.30 DRILL

$\frac{3}{16}$ DRILL

$\frac{1}{8}$

$\frac{5}{16}$

$\frac{17}{32}$

$\frac{7}{32}$

$\frac{7}{16}$

$\frac{1}{8}$

$\frac{3}{16}$

$\frac{3}{8}$

$1\frac{29}{32}$

$\frac{3}{16}$

$\frac{3}{8}$

$\frac{11}{16}$

$\frac{13}{16}$

| SHAFT SUPPORT | R.CAMPBELL | SCALE: 1" = 1" | B-11 |

75
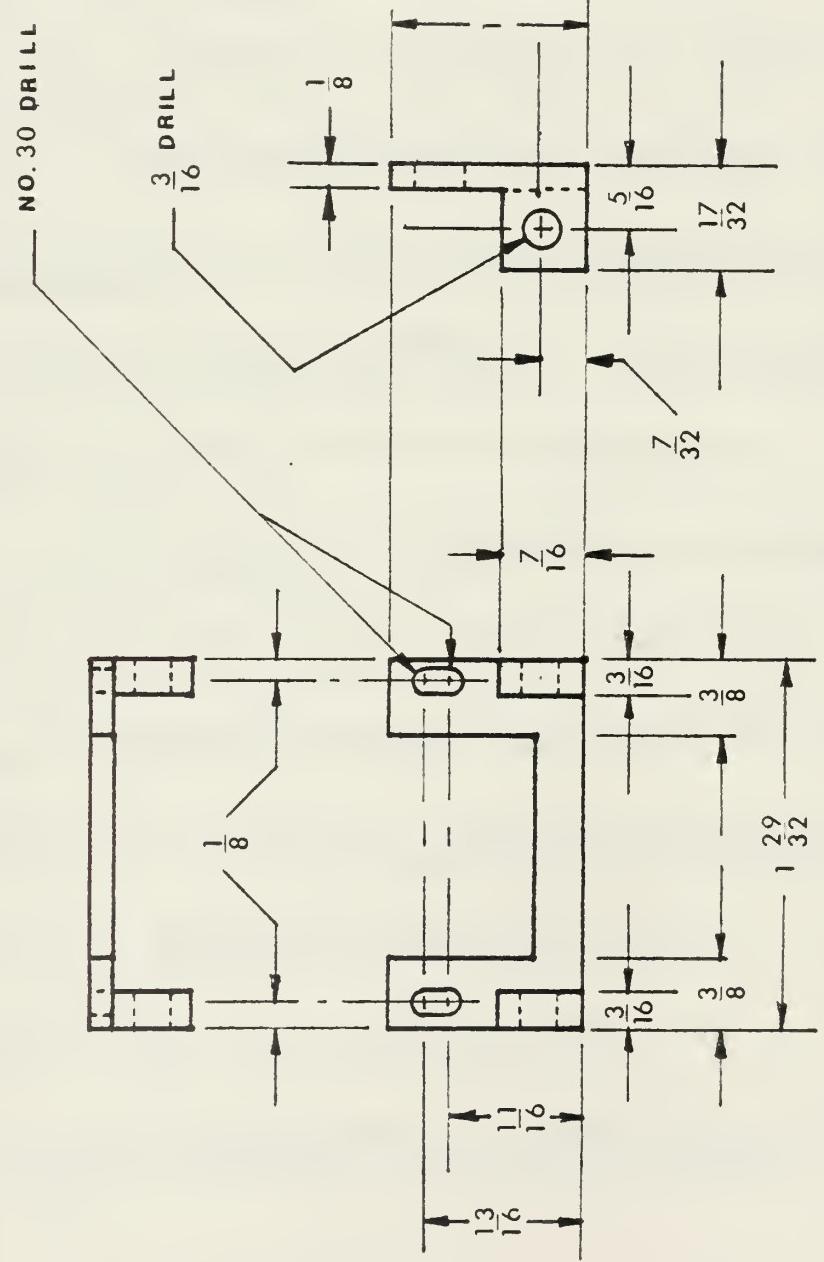
LIST OF REFERENCES

1. Black, P.H. and Adams Jr., O.E., <u>Machince Design</u>, McGraw-Hill, 1968.

2. Cambridge Scientific Instruments Limited TL 1057-TM-96113/8, <u>Steroscan Multipurpose Specimen Stage</u>, issue 4, George Kent Group, Unkn.

3. Gieseche, F.E., Mithcell, A., Spencer, H.C. and Hill, J.L., <u>Technical Drawing</u>, 5th ed., MacMillan Co., 1967.

4. Holman, J.P., <u>Experimental Methods for Engineers</u>, McGraw-Hill, 1978.

5. Leeds and Northrup Co., 077989 issue 2, <u>Conversion Tables for Thermocouples</u>, p. 18, Leeds and Northrup Co., 1977.

6. Magnaflux Corporation Catalog ESA-SG1-A, <u>Strain Gages</u>, p. 2-5, Magnaflux Corporation, 1973.

7. North American Rockwell Catalog 60, <u>Boston Gear</u>, p. 101-105, Boston Gear Works, 1969.

8. Peckner, D. and Bernstein, I.M., <u>Handbook of Stainless Steels</u>, p. 13-9, McGraw-Hill, 1977.

9. Pilkey, W.D. and Pilkey, O.H., <u>Mechanics of Solids</u>, pp. 2.5, 237-]39, McGraw-Hill, 1977.

10. Shigley, J.E., <u>Mechanical Engineering Design,</u> 3rd ed., McGraw-Hill, 1977.

11. The Aluminum Association Inc., <u>Aluminum Standards and Data</u>, 4th ed., p. 107, The Aluminum Association Inc., 1974.

12. Van Valck, L.H. <u>Elements of Materials Science</u>, p. 420, Addison-Wesley, 1964.

13. Watlow Corporation, <u>Watlow Bulletin #100</u>, 679F ed., Watlow Corp., 1979.

14. Wayman, C.M., <u>Some Applications of Shape-Memorey Alloys</u>, paper presented at University of Illinois, Urbana, Illinois, 1978.

INITIAL DISTRIBUTION LIST

No. Copies

1. Defense Technical Information Center   2
   Cameron Station
   Alexandria, Virginia 22314

2. Library, Code 0142   2
   Naval Postgraduate School
   Monterey, California 93940

3. Department Chairman, Code 69   1
   Department of Mechanical Engineering
   Naval Postgraduate Schoo;
   Monterey, California 93940

4. Professor Jeff Perkins, Code 69Ps   1
   Department of Mechanical Engineering
   Naval Postgraduate School
   Monterey, California 93940

5. Professor G. Vanderplaats, Code 69Vn   1
   Department of Mechanical Engineering
   Naval Postgraduate School
   Monterey, California 93940

6. LCDR Richard Campbell, USN   1
   Route 1, Box 411
   Las Lunas, New Mexico 87109